The Plant Cell, Vol. 26: 2168–2183, May 2014, www.plantcell.org

In Planta Recognition of a Double-Stranded RNA Synthesis Protein Complex by a Potexviral RNA Silencing Suppressor[C][W][OPEN]

Yukari Okano, Hiroko Senshu, Masayoshi Hashimoto, Yutaro Neriya, Osamu Netsu, Nami Minato, Tetsuya Yoshida, Kensaku Maejima, Kenro Oshima, Ken Komatsu, Yasuyuki Yamaji, and Shigetou Namba[1]

Laboratory of Plant Pathology, Graduate School of Agricultural and Life Sciences, The University of Tokyo, Bunkyo-ku, Tokyo 113-8657, Japan

RNA silencing plays an important antiviral role in plants and invertebrates. To counteract antiviral RNA silencing, most plant viruses have evolved viral suppressors of RNA silencing (VSRs). TRIPLE GENE BLOCK PROTEIN1 (TGBp1) of potexviruses is a well-characterized VSR, but the detailed mechanism by which it suppresses RNA silencing remains unclear. We demonstrate that transgenic expression of TGBp1 of plantago asiatica mosaic virus (PlAMV) induced developmental abnormalities in *Arabidopsis thaliana* similar to those observed in mutants of SUPPRESSOR OF GENE SILENCING3 (SGS3) and RNA-DEPENDENT RNA POLYMERASE6 (RDR6) required for the *trans*-acting small interfering RNA synthesis pathway. PlAMV-TGBp1 inhibits SGS3/RDR6-dependent double-stranded RNA synthesis in the *trans*-acting small interfering RNA pathway. TGBp1 interacts with SGS3 and RDR6 and coaggregates with SGS3/RDR6 bodies, which are normally dispersed in the cytoplasm. In addition, TGBp1 forms homooligomers, whose formation coincides with TGBp1 aggregation with SGS3/RDR6 bodies. These results reveal the detailed molecular function of TGBp1 as a VSR and shed new light on the SGS3/RDR6-dependent double-stranded RNA synthesis pathway as another general target of VSRs.

INTRODUCTION

Sequence-specific RNA degradation in RNA silencing plays an important antiviral role in plants and invertebrates (Ding and Voinnet, 2007). Previous studies have identified a variety of factors involved in this antiviral mechanism, triggered by double-stranded RNA (dsRNA) intermediates of cytoplasmically replicating viruses or structured regions of viral RNA. In plants, dsRNAs are processed by DICER-LIKE (DCL) RNase III enzymes into small 21- to 24-nucleotide products termed virus-derived small interfering RNAs (vsiRNAs). In *Arabidopsis thaliana*, DCL4, DCL2, and DCL3 produce 21-, 22-, and 24-nucleotide vsiRNAs, respectively, in a hierarchical and redundant manner (Blevins et al., 2006; Deleris et al., 2006; Diaz-Pendon et al., 2007). vsiRNAs incorporated into an RNA-induced silencing complex (RISC) containing ARGONAUTE1 (AGO1), one of 10 AGO proteins that possess ribonuclease activity, lead to cleavage of homologous RNAs (Morel et al., 2002; Baumberger and Baulcombe, 2005; Wang et al., 2011).

Antiviral RNA silencing in plants can be partitioned into three phases: initiation, amplification, and systemic spread (Ding and Voinnet, 2007). Once RNA silencing is initiated in a plant cell with the production of primary vsiRNAs from dsRNAs, it can be amplified through a process referred to as transitive silencing. During this amplification phase, viral RNA fragments generated by primary vsiRNA- and RISC-mediated cleavage serve as a template for the host SUPPRESSOR OF GENE SILENCING3 (SGS3)/RNA-DEPENDENT RNA POLYMERASE6 (RDR6) complex to produce de novo dsRNA, which is subsequently processed into 21-nucleotide secondary vsiRNAs by DCL4 (Wang et al., 2011). Indeed, accumulation of cucumber mosaic cucumovirus (CMV) is markedly increased in *Arabidopsis rdr6* or *sgs3* mutants, indicating that amplification of RNA silencing plays an important role in antiviral defense (Wang et al., 2011). Furthermore, amplification of RNA silencing has been implicated in the spread of an RNA silencing signal (Himber et al., 2003; Schwach et al., 2005; Kalantidis et al., 2008). This signal can move between cells via plasmodesmata and over long distances through phloem, triggering sequence-specific RNA silencing in distant tissues (Voinnet and Baulcombe, 1997; Voinnet et al., 1998). This signal can prime antiviral RNA silencing in surrounding naive cells prior to viral infection (Schwach et al., 2005). The requirement of RDR6 for systemic movement of a silencing signal suggests that amplification of RNA silencing is involved in antiviral defense in uninfected systemic tissues.

In addition to its antiviral role, RNA silencing in plants plays essential roles in endogenous biological processes such as plant development, maintenance of genome stability, and response to environmental stresses. These processes are mediated by endogenous 21- to 24-nucleotide small RNAs (sRNAs) such as microRNA (miRNA), *trans*-acting small interfering RNA (tasiRNA), and natural antisense small interfering RNA. miRNAs are processed

[1] Address correspondence to anamba@mail.ecc.u-tokyo.ac.jp.
The author responsible for distribution of materials integral to the findings presented in this article in accordance with the policy described in the Instructions for Authors (www.plantcell.org) is: Shigetou Namba (anamba@mail.ecc.u-tokyo.ac.jp).
[C] Some figures in this article are displayed in color online but in black and white in the print edition.
[W] Online version contains Web-only data.
[OPEN] Articles can be viewed online without a subscription.
www.plantcell.org/cgi/doi/10.1105/tpc.113.120535

from imperfect stem-loop regions of long primary transcripts of miRNA genes by DCL1 (Bartel, 2004). tasiRNAs are generated from noncoding TAS transcripts after miRNA-mediated cleavage by AGO1/miRNA or AGO7/miRNA complexes (Montgomery et al., 2008a, 2008b). The cleaved fragment is then stabilized by SGS3 and converted into dsRNA by RDR6. The resulting dsRNA is sequentially processed by DCL4 into a 21-nucleotide tasiRNA (Peragine et al., 2004; Nakazawa et al., 2007). The tasiRNA is incorporated into AGO1-loaded RISC to guide sequence-specific cleavage of the target mRNA. Thus, despite their functional differences, antiviral and tasiRNA silencing pathways share common components such as RDR6, SGS3, and DCL4.

To counteract antiviral RNA silencing, the majority of plant viruses have evolved viral suppressors of RNA silencing (VSRs). The most common strategies to suppress RNA silencing by VSRs are double-stranded small interfering RNA (siRNA) sequestration and interaction with AGO1. Tombusviral p19 protein sequesters siRNA duplexes and inhibits their loading into a RISC (Vargason et al., 2003; Ye et al., 2003), and several VSRs also suppress RNA silencing through direct binding to siRNAs (Lakatos et al., 2006; Mérai et al., 2006). On the other hand, sweet potato mild mottle virus P1 protein and turnip crinkle virus P38 protein prevent RISC assembly through a physical interaction with AGO1 by mimicking as yet unidentified Gly/Trp host proteins required for RISC function (Azevedo et al., 2010; Giner et al., 2010). Moreover, CMV 2b protein inhibits AGO1 activity through a physical interaction with its PAZ and PIWI domains (Zhang et al., 2006). Furthermore, beet western yellows virus P0 protein and cymbidium ringspot virus (CymRSV) p19 protein can decrease the accumulation of AGO1 protein (Baumberger et al., 2007; Bortolamiol et al., 2007; Várallyay et al., 2010). Thus, siRNA binding and AGO1 inactivation have been regarded as general mechanisms of RNA silencing suppression and studied in detail. However, few studies have identified VSRs that target other components in the RNA silencing pathway, especially during the amplification step involving RDR6, SGS3, and DCL4. siRNA binding VSRs and AGO1-targeting VSRs are known to interfere with (as a side effect) endogenous RNA silencing pathways (Kasschau et al., 2003; Chapman et al., 2004; Dunoyer et al., 2004; Zhang et al., 2006; Moissiard et al., 2007). For example, siRNA binding VSRs such as the p19 protein also bind miRNA and tasiRNA duplexes, thereby preventing RISC assembly (Chapman et al., 2004; Moissiard et al., 2007). Moreover, AGO1-targeting VSRs such as the 2b protein increase the accumulation of miRNA- or tasiRNA-targeted mRNAs (Zhang et al., 2006). In agreement with these findings, transgenic plants expressing a VSR often show developmental defects. Therefore, the morphological symptoms caused by plant viruses such as stunt, proliferation, leaf crinkle, and leaf curl are generally assumed to be consequences of perturbing endogenous RNA silencing by VSRs.

The TRIPLE GENE BLOCK PROTEIN1 (TGBp1) of potato X potexvirus (PVX), the type species of the genus *Potexvirus*, is a well-characterized VSR used for various analyses similar to the tombusviral p19 and potyviral HC-Pro. However, the detailed mechanism by which TGBp1 suppresses RNA silencing remains unclear, likely due to the low silencing suppression activity of PVX TGBp1. Indeed, PVX was not originally thought to encode a VSR, because PVX did not suppress RNA silencing during viral infection (Brigneti et al., 1998; Voinnet et al., 1999). Nevertheless, subsequent studies showed that PVX TGBp1 suppresses RNA silencing of the green fluorescent protein (GFP) gene in agroinfiltrated leaves (local silencing) and spread of the silencing into upper noninoculated tissues in GFP transgenic plants (systemic silencing) (Voinnet et al., 2000). In a previous study, we showed that the levels of RNA silencing suppressor activity differ depending on the virus species and that of PVX is relatively low among potexviruses (Senshu et al., 2009).

Therefore, we used the TGBp1 of plantago asiatica mosaic virus (PlAMV), which shows much higher suppressor activity than PVX, to investigate the mechanism by which potexvirus TGBp1 suppresses RNA silencing. Using PlAMV-TGBp1 transgenic *Arabidopsis*, we showed that TGBp1 inhibits RDR6/SGS3-dependent dsRNA synthesis in plants. Further functional analysis of TGBp1 showed that TGBp1 interacts with SGS3 and RDR6 to coaggregate and enwrap SGS3-containing bodies (SGS3/RDR6 bodies). These results revealed the detailed molecular function of TGBp1 as a VSR and shed new light on the SGS3/RDR6-dependent dsRNA synthesis pathway as another general target of VSRs.

RESULTS

In *Arabidopsis*, TGBp1 Induces Developmental Defects Resembling Those Observed in tasiRNA-Deficient Mutants

To identify the component that TGBp1 inhibits in the antiviral RNA silencing pathway, we observed the phenotype of the TGBp1 transgenic *Arabidopsis*. As described previously, *Arabidopsis* transformants expressing p19 of tomato bushy stunt tombusvirus (TBSV) and 2b of CMV exhibited severe developmental defects in both leaves and flowers (Figure 1A; Chapman et al., 2004; Zhang et al., 2006). Approximately 60% (27 of 46) of TGBp1 transformants (1F, 7A, and 10D) had downward-curled leaf margins compared with wild-type Columbia-0 (Col-0) or β-glucuronidase (GUS) transformants (Figure 1A). However, no developmental defects occurred in other organs, including seeds, although flowers tended to bloom earlier. Immunoblot analysis showed that extensive expression of TGBp1 was detected in transgenic lines with severe curled phenotypes (1F, 7A, and 10D), while low levels of TGBp1 expression were detected in a line with a mild phenotype (7D), indicative of a correlation between the phenotype and expression of the TGBp1 protein (Figure 1B). Downward curling of leaf margins is a characteristic phenotype of tasiRNA-deficient mutants such as *sgs3*, *rdr6*, *dcl4*, and *ago7* (Figure 1A; Adenot et al., 2006), suggesting that TGBp1 may prevent some specific steps in the tasiRNA pathway.

TGBp1 Significantly Reduces tasiRNA Accumulation

To examine the effects of TGBp1 on sRNA accumulation, we performed deep sequencing of sRNA populations extracted from TGBp1 and GUS transformants and compared them (Supplemental Table 1). The normalized, size-specific distribution of sRNAs showed a significant increase in the proportion of 23- and 24-nucleotide sRNAs and a decrease in the proportion of 21-nucleotide sRNAs in TGBp1 transformants compared with GUS

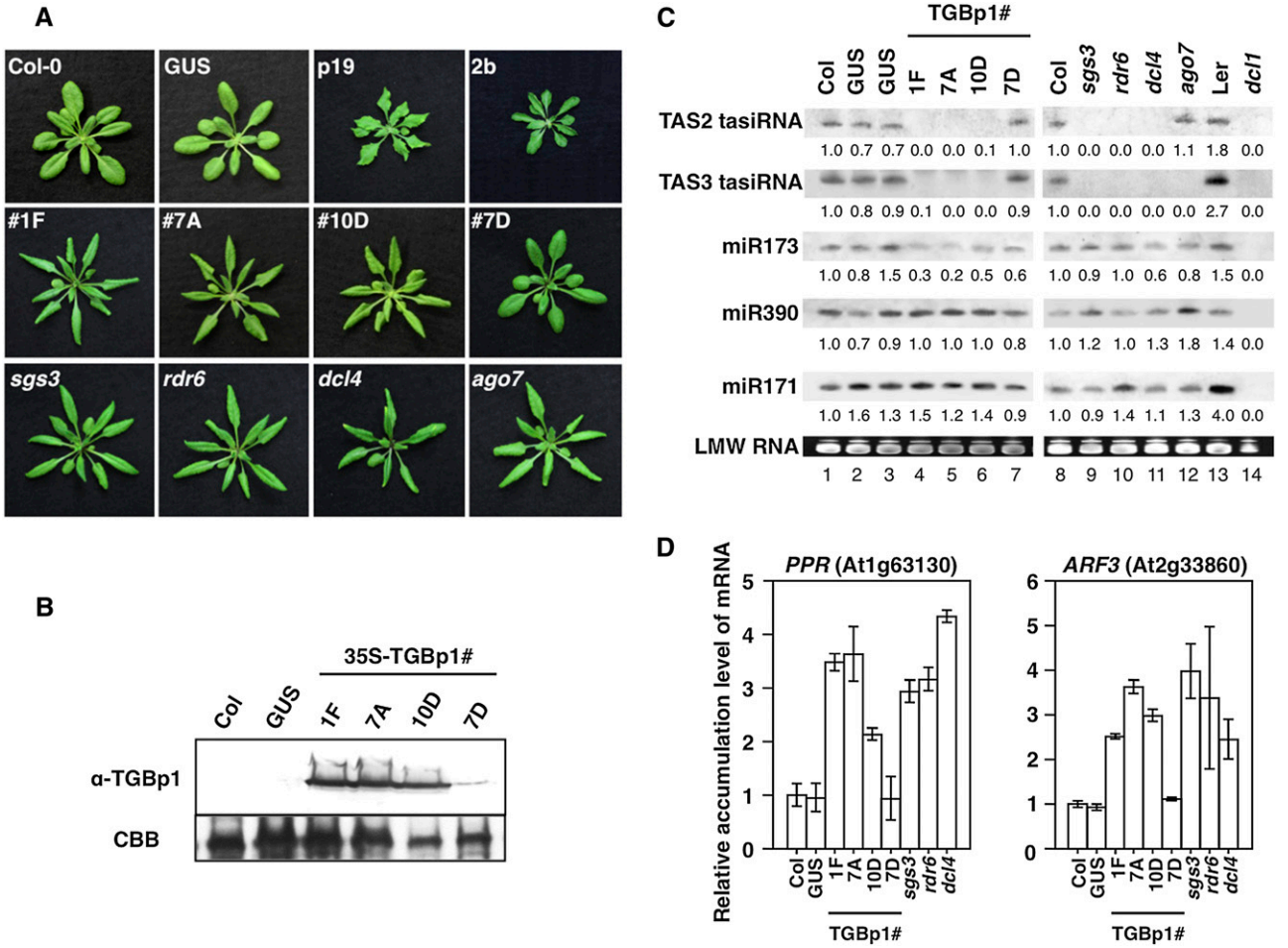

Figure 1. TGBp1 Induces Developmental Defects Resembling Those Observed in tasiRNA-Deficient Mutants and Significantly Reduces tasiRNA Accumulation.

(A) Photographs of 4-week-old TGBp1 transgenic lines (1F, 7A, 10D, and 7D), tasiRNA-deficient mutants (*sgs3*, *rdr6*, *dcl4*, and *ago7*), TBSV p19, CMV 2b, and GUS transformants, and a wild-type Col-0 plant.

(B) Immunoblot analysis with anti-TGBp1 polyclonal antibody to detect TGBp1 protein levels in ~5-week-old TGBp1 transgenic lines. Coomassie Brilliant Blue (CBB) staining is shown as a loading control.

(C) RNA gel blot analysis of TAS2 and TAS3 tasiRNAs, miR173, miR390, and miR171. Total RNA was prepared from the indicated transformants or mutants. The numbers below each lane show accumulation levels relative to wild-type Col-0, after normalization against ethidium bromide–stained low-molecular-weight (LMW) RNAs.

(D) Quantitative real-time RT-PCR analysis of *PPR* and *ARF3* mRNA levels in plants at the reproductive stage. Relative expression values (means ± SD, $n = 3$) were normalized against *ACTIN2* mRNA levels.

[See online article for color version of this figure.]

transformants (Supplemental Figure 1). miRNAs were differentially regulated, because 88 miRNAs were upregulated more than twice and 75 miRNAs were downregulated less than one-half in TGBp1 transformants compared with GUS transformants (Supplemental Data Set 1). Levels of 41 miRNAs were not changed significantly. Remarkably, we found that all the tasiRNA family members, including TAS1a, TAS1b, TAS1c, TAS2, TAS3a, TAS3b, TAS3c, and TAS4 tasiRNAs, showed significant decreases in TGBp1 transformants (Supplemental Table 2). These results indicated that TGBp1 decreased the accumulation of tasiRNAs but did not exert a uniform effect on the populations of miRNAs.

To confirm the deep sequencing result and examine the effects of TGBp1 on the tasiRNA pathway, we investigated the accumulation of tasiRNA pathway-related sRNAs in TGBp1 transformants, including tasiRNAs and miRNAs required for cleavage of the initial transcripts of TAS genes (miR173 for TAS1 and TAS2 and miR390 for TAS3) (Allen and Howell, 2010). RNA gel blot analysis revealed that TAS2 and TAS3 tasiRNAs were significantly decreased or undetectable in severe TGBp1 transformants (1F, 7A, and 10D) but readily detectable in a mild transformant (7D) (Figure 1C). This decrease of tasiRNAs was similar to those in *sgs3*, *rdr6*, and *dcl4* reported previously (Figure 1C; Xie et al.,

2005; Yoshikawa et al., 2005). miR173, an initiator of TAS1 and TAS2 tasiRNA production, was decreased to some extent in severe TGBp1 transformants; however, we observed no effect on miR390, an initiator of TAS3 tasiRNA production, or on miR171, a control miRNA (Figure 1C). In tasiRNA-deficient mutants (*sgs3*, *rdr6*, *dcl4*, and *ago7*), the levels of miR173, miR390, and miR171 were not significantly altered (Figure 1C, lanes 8 to 12). The specific decrease of TAS3 tasiRNA in *ago7* was also reproduced, indicating that AGO7 is involved in TAS3 tasiRNA production, as described previously (Figure 1C, lane 12) (Allen and Howell, 2010). These results were consistent with the deep sequencing result that TGBp1 caused a uniform decrease in the accumulation of tasiRNAs but not in the accumulation of miRNAs.

We next investigated whether the reduced tasiRNA accumulation in TGBp1 transformants affected their target mRNAs. Levels of *PPR* (At1g63130) and *ARF3* (At2g33860) mRNAs, targets of TAS2 and TAS3 tasiRNAs (Montgomery et al., 2008a, 2008b), were elevated 2.1 to 3.6 and 2.5 to 3.6 times, respectively, in TGBp1 high-expression lines (1F, 7A, and 10D) compared with wild-type Col-0 (Figure 1D). These elevations were comparable to *PPR* and *ARF3* mRNA levels in *sgs3*, *rdr6*, and *dcl4* mutants, 2.9 to 4.3 and 2.4 to 4.0 times higher, respectively. These results suggested that TGBp1-mediated inhibition of tasiRNA accumulation increased the accumulation of tasiRNA target mRNAs.

TGBp1 Does Not Affect miRNA-Directed Cleavage of TAS Transcripts

To examine which step of the tasiRNA biosynthesis pathway TGBp1 inhibits, we first investigated whether miRNA-guided primary cleavage of TAS transcripts occurred in TGBp1-expressing plants. Considering that miR173, an initiator of TAS1 and TAS2 tasiRNA, was decreased to some degree in TGBp1 transformants while miR390, an initiator of TAS3 tasiRNA, was not affected (Figure 1C), it is still possible that the inhibition of tasiRNA synthesis by TGBp1 is caused by the reduced efficiency of primary cleavage of the TAS transcript. Thus, we performed RNA ligase–mediated 5′ rapid amplification of cDNA ends (RLM-5′ RACE) PCR (Liu and Gorovsky, 1993) to detect the 3′ cleavage products of the primary TAS transcripts. In wild-type Col-0 and GUS transformants, primary cleavage products of TAS2 and TAS3 precursors guided by miR173 and miR390, 313 and 77 bp, respectively, were nearly undetectable (Figures 2A and 2B, lanes 1 and 2). This may be because these cleaved products are immediately converted to dsRNA and subsequently processed to tasiRNA (Yoshikawa et al., 2005). Instead, in these control plants, we detected a band corresponding to a secondary 3′ cleavage product from the TAS3 transcript, guided by TAS3 tasiRNA (110 bp) (Figures 2A and 2B, lanes 1 and 2; Allen et al., 2005; Montgomery et al., 2008a). In the tasiRNA-deficient mutants *rdr6* and *dcl4*, the primary 3′ cleavage products, 313 and 77 bp, were detected while the secondary cleavage product, 110 bp, was not (Figure 2B, lanes 7 and 8), indicating that they are involved in downstream steps of the tasiRNA pathway, dsRNA synthesis, and processing of dsRNA, respectively. Similar to these mutants, the primary 3′ cleavage products, 313 and 77 bp, were detectable in TGBp1 transformants while the secondary 3′ cleavage product, 110 bp, was not (Figure 2B, lanes 3 to 5). These results were confirmed by RNA gel blot analysis detecting the primary TAS2 transcript and its cleavage products (Supplemental Figure 2). In wild-type Col-0 and GUS-expressing plants, the 5′ cleavage product of the TAS2 precursor was detected but the 3′ cleavage product was not, while both the 5′ and 3′ cleavage products were detected in TGBp1 transformants as well as in *rdr6* mutants. These findings were consistent with the results of the RLM-5′ RACE PCR assay. We noted that both the 5′ and 3′ cleavage products were absent in the *sgs3* mutant, indicating that SGS3 stabilizes the cleavage products, as reported previously (Yoshikawa et al., 2005; Elmayan et al., 2009). Considering these results, TGBp1 is likely to block downstream steps in tasiRNA synthesis, such as RDR6-mediated dsRNA synthesis or DCL4-mediated processing of dsRNA to tasiRNA.

TGBp1 Inhibits dsRNA Synthesis

To further analyze whether TGBp1 blocks dsRNA synthesis, the conversion of miRNA-cleaved TAS fragments into dsRNA by SGS3/RDR6, we performed RNase protection assays (Zheng et al., 2010) to detect dsRNA. While in both TAS2 and TAS3 panels, DNA bands were detected even after treatment with RNase I in *dcl4* mutants, indicating the existence of dsRNA, those bands were not detected in TGBp1 transformants or in wild-type Col-0 and *rdr6* mutants (Figure 2C). These results suggest that dsRNA exists in *dcl4* but not in TGBp1 transformants, *rdr6*, and Col-0 plants. The absence of dsRNAs in Col-0 was because they are immediately processed into tasiRNAs in the presence of DCL4, as reported previously (Yoshikawa et al., 2005). These results were confirmed by RNA gel blot analysis detecting the complementary RNA of TAS2, indicating the existence of dsRNA. The complementary RNA accumulated only in the *dcl4* mutants and not in wild-type Col-0 plants, *rdr6* mutants, or TGBp1 transformants (Figure 2D). These results indicate the absence of dsRNA in TGBp1 transformants, but the possibility remains that dsRNAs are synthesized but rapidly processed into tasiRNAs by DCL4. However, this seems unlikely, because the accumulation of tasiRNAs was nearly undetectable in TGBp1 transformants. Collectively, these data suggest that TGBp1 inhibits dsRNA synthesis in the tasiRNA biogenesis pathway.

TGBp1 Interacts with SGS3 and RDR6 in Planta

Since SGS3 and RDR6 are involved in dsRNA synthesis in the tasiRNA biogenesis pathway (Allen and Howell, 2010), we investigated whether TGBp1 targets these factors. We first performed coimmunoprecipitation immunoblot analyses to determine whether TGBp1 interacts with SGS3 and RDR6. When SGS3-3myc and Flag-RDR6 were transiently expressed in *Nicotiana benthamiana* leaves via agroinfiltration and coimmunoprecipitation immunoblot analyses were conducted on total proteins from infiltrated leaves, SGS3-3myc was detected in Flag-RDR6 immunoprecipitates, indicative of an interaction between SGS3 and RDR6, as reported previously (Figure 3A, lane 12; Kumakura et al., 2009). Similarly, TGBp1-3myc coimmunoprecipitated with both Flag-SGS3 and Flag-RDR6 (Figure 3A, lanes 9 and 11, respectively). These results showed that TGBp1 interacts with both SGS3 and RDR6.

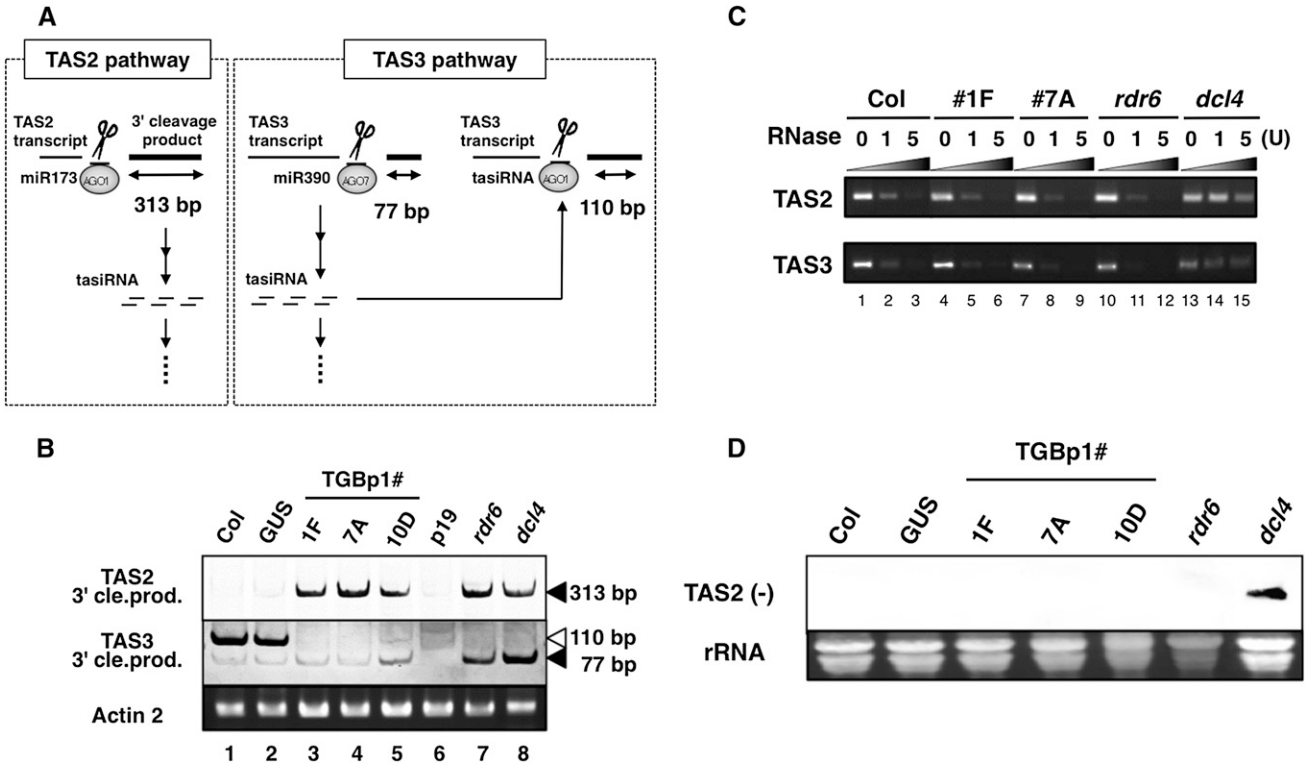

Figure 2. TGBp1 Does Not Affect miRNA-Directed Cleavage of the TAS Transcripts but Represses dsRNA Synthesis.

(A) Schematic representation of detection of the 3′ cleavage products (thick lines) of the primary TAS transcripts using RLM-5′ RACE PCR. In the TAS2 pathway, a 313-bp product generated from the TAS2 primary transcript by the AGO1/miR173 complex could be detected. In the TAS3 pathway, a 77-bp product generated from the TAS3 primary transcript by the AGO7/miR390 complex, as well as a 110-bp product generated by the AGO1/TAS3 tasiRNA [5′D2(–)] complex, could be detected.

(B) RLM-5′ RACE PCR analysis of the 3′ cleavage product of the primary TAS2 and TAS3 transcripts in wild-type Col-0 plants, GUS transformants, the TGBp1 transgenic lines, the p19 transformants, and the *rdr6* and *dcl4* mutants at the reproductive stage. Black and white arrowheads indicate the bands corresponding to the 3′ cleavage product generated from the TAS primary transcript by the AGO/miRNA complex and that generated from the TAS3 primary transcript by the AGO1/TAS3 tasiRNA [5′D2(–)] complex, respectively. *ACTIN2* was used as a control.

(C) Detection of double-stranded TAS2 and TAS3 RNAs using the RNase protection assay. Total RNAs were treated with DNase I and subsequently treated with 0, 1, and 5 units (U) of RNase I, which digests single-stranded RNA and leaves dsRNA intact, followed by RT-PCR amplification.

(D) RNA gel blot analysis performed on 20 μg of a high-molecular-weight RNA fraction from plants at the reproductive stage to detect complementary RNA derived from the TAS2 transcript. Relative gel loadings are shown by ethidium bromide staining of rRNA.

We further analyzed these interactions in vivo using bimolecular fluorescence complementation (BiFC) assays in transiently transformed *N. benthamiana* epidermal cells. Coexpression of TGBp1-YFP^N and SGS3-YFP^C led to the generation of intracellular fluorescent aggregates of varying sizes and forms (Figure 3B, left panel). Closer observation at higher magnification revealed that the aggregates were composed of minute vesicles (Figure 3B, right panel). These results demonstrated that TGBp1 interacts with SGS3. We also investigated the interaction between TGBp1 and RDR6 by BiFC but were unable to detect any yellow fluorescent protein (YFP) fluorescence (Supplemental Figures 3A and 3B). Moreover, coexpression of RDR6-YFP^N and SGS3-YFP^C failed to reconstitute YFP fluorescence, although the interactions between RDR6 and TGBp1 or SGS3 were demonstrated by the coimmunoprecipitation analysis (Figure 3A). Taking these findings into consideration, the interaction between RDR6 and TGBp1 or SGS3 may be below the detection limits of BiFC due to the low expression levels of RDR6 in plants.

TGBp1 Alters the Subcellular Localization of SGS3

Next, we examined the subcellular localization of TGBp1, SGS3, and RDR6. When YFP-tagged SGS3 (SGS3-YFP) was expressed in *N. benthamiana* leaves via agroinfiltration, the signals localized in discrete granules in the cytoplasm (Figures 4A and 4B). Based on their size (~2 to 8 μm in diameter), shape, and cytoplasmic localization, these granules were likely to be SGS3/RDR6 bodies, as reported previously (Kumakura et al., 2009). We next attempted to express RDR6-YFP in *N. benthamiana* leaves but failed to detect any signal (Supplemental Figures 3C and 3D), presumably due to the low expression level of RDR6-YFP. Cyan fluorescent protein (CFP)-tagged TGBp1 (TGBp1-CFP) localized to the cell periphery and to the nucleus (Figure 4C). Closer observation at

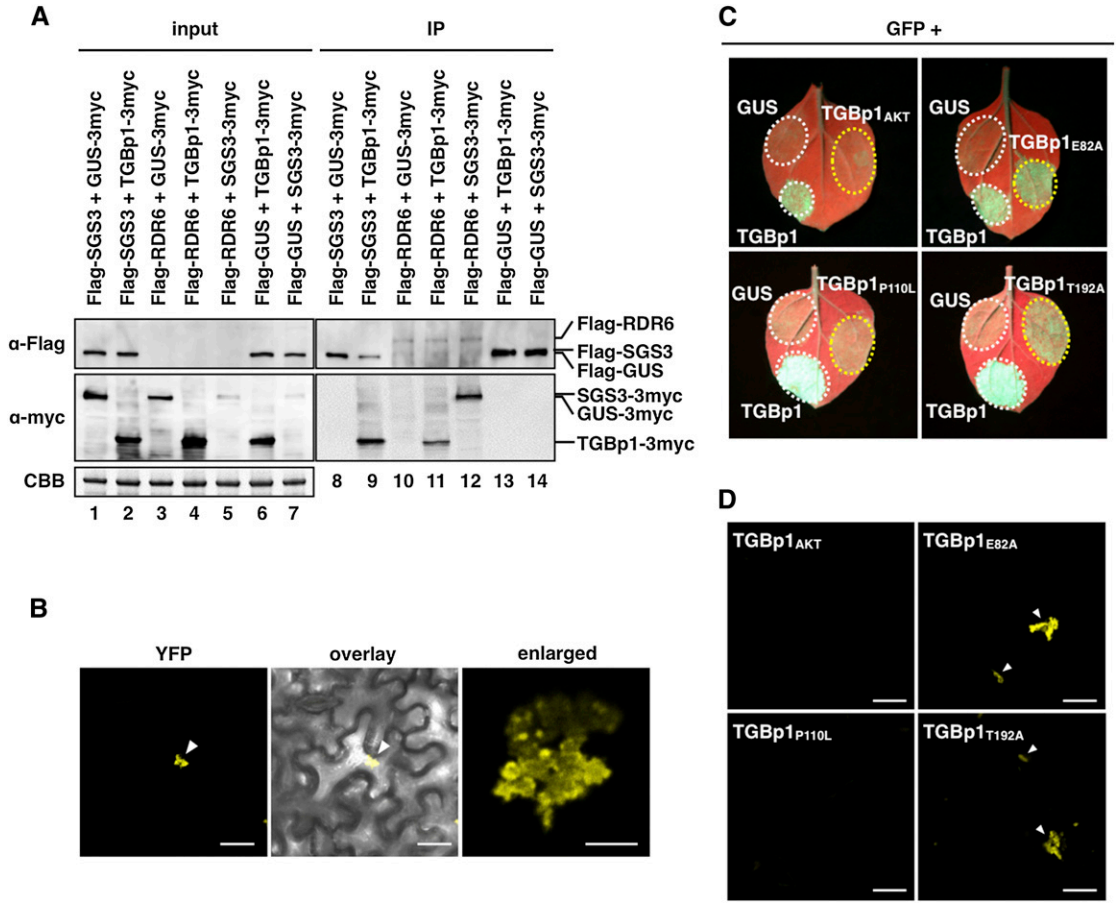

Figure 3. TGBp1 Interacts with RDR6 and SGS3 in Planta.

(A) Coimmunoprecipitation immunoblot analyses. Dual combinations of SGS3, RDR6, and GUS tagged with Flag epitope and those tagged with triple c-myc epitope were coexpressed in *N. benthamiana* leaves. Coimmunoprecipitation analyses were performed by using anti-Flag antibody, and the input and immunoprecipitated (IP) proteins were analyzed by immunoblot analysis using anti-Flag (α-Flag) and anti-myc (α-myc) antibodies. Coomassie Brilliant Blue (CBB) staining is shown as a loading control.

(B) BiFC assays between TGBp1 and SGS3. TGBp1-YFP^N and SGS3-YFP^C were coexpressed by agroinfiltration in leaf epidermal cells of *N. benthamiana* plants. The left panel shows a YFP fluorescence image showing the generation of the intracellular fluorescent aggregate (arrowhead). The middle panel shows an overlay of a bright-field image and the left panel. The right panel shows a higher magnification view of the left panel, showing the aggregate composed of minute vesicles. Bars in the left and middle panels = 25 μm; bar in the right panel = 5 μm.

(C) *Agrobacterium*-mediated RNA silencing suppression assay of TGBp1 mutants. Wild-type *N. benthamiana* leaves were coinfiltrated with *Agrobacterium* mixtures containing a vector expressing GFP and GUS (top left patches of each panel), wild-type TGBp1 (bottom left patches), or TGBp1 mutant (TGBp1$_{AKT}$, TGBp1$_{E82A}$, TGBp1$_{P110L}$, and TGBp1$_{T192A}$; right patches) expression vectors. GFP fluorescence was visualized under UV light at 4 d after inoculation.

(D) BiFC assay to detect the interaction between TGBp1 mutants and SGS3. SGS3-YFP^N and TGBp1$_{AKT}$-YFP^C, TGBp1$_{E82A}$-YFP^C, TGBp1$_{P110L}$-YFP^C, or TGBp1$_{T192A}$-YFP^C were coexpressed in leaf epidermal cells of *N. benthamiana* plants. Arrowheads indicate the intracellular fluorescent aggregates. Bars = 25 μm.

higher magnification of the peripheral areas of the cell showed that fluorescence was also visible as puncta embedded in the cell walls (Figure 4D). These punctate structures colocalized with PDLP1-YFP (Amari et al., 2011), indicating the localization in plasmodesmata (Supplemental Figures 4A to 4C). Moreover, TGBp1-CFP was also localized throughout the entire nucleus with punctate structures and formed aggregates adjacent to the nucleus (Figure 4E; Supplemental Figures 4D to 4F).

Next, we coexpressed SGS3-YFP and TGBp1-CFP and examined whether coexpression of both proteins affected their subcellular localization. Unexpectedly, SGS3-YFP bodies, which were dispersed in the cytoplasm when expressed alone, gathered together when coexpressed with TGBp1-CFP (Figure 4F; Supplemental Figure 4G). TGBp1-CFP, which localized to the nucleus, cytoplasm, and plasmodesmata when expressed alone, formed large amorphous aggregates in the cytoplasm when

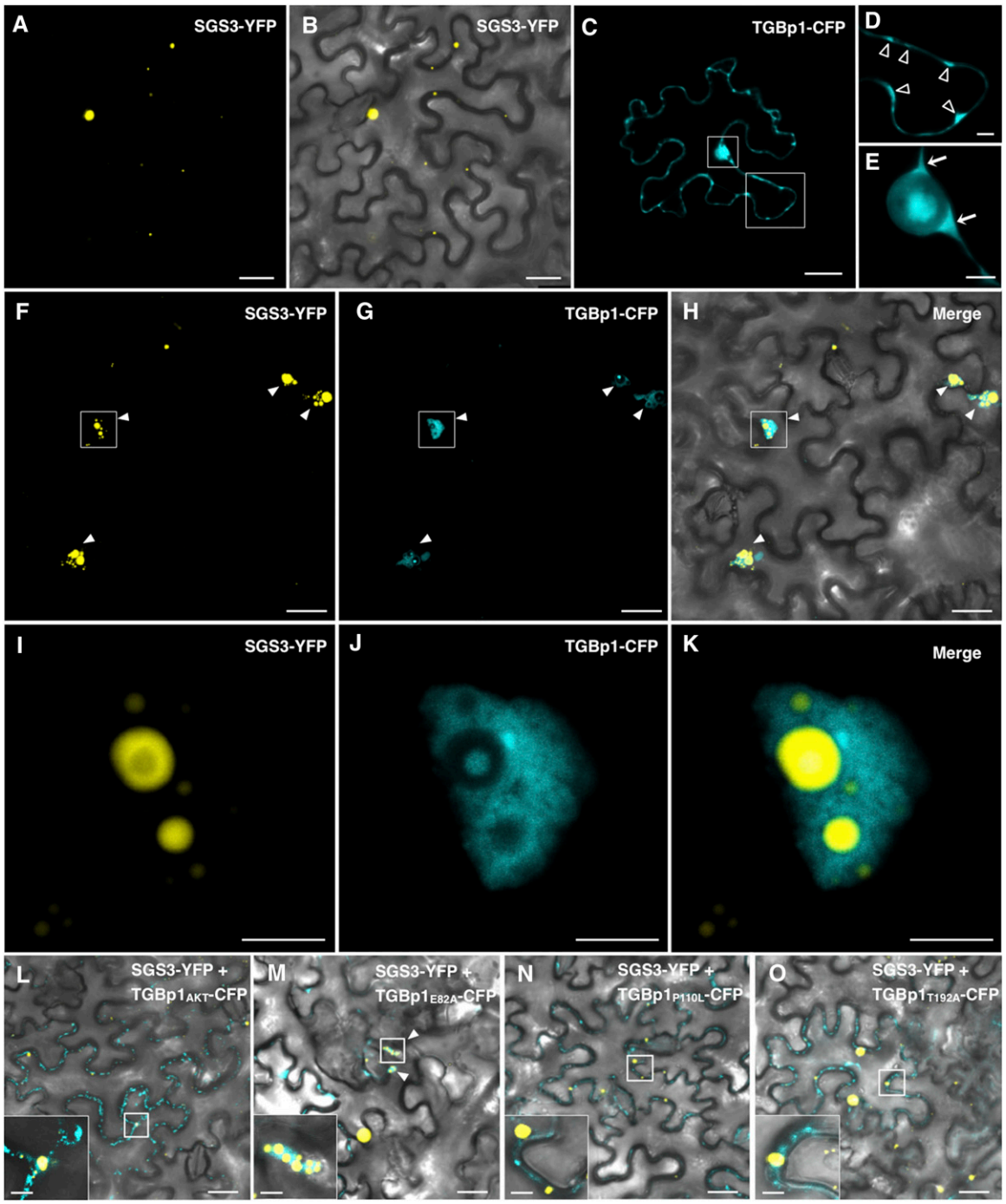

Figure 4. TGBp1 Alters the Subcellular Localization of SGS3.

(A) to **(E)** Confocal sections of *N. benthamiana* leaves expressing SGS3-YFP alone (**[A]** and **[B]**) or TGBp1-CFP alone (**[C]** to **[E]**). **(B)** shows an overlay of a bright-field image and the fluorescence image of **(A)**. **(D)** shows a higher magnification view of lower right boxed region in **(C)**. The arrowheads in **(D)** indicate puncta embedded in cell walls. **(E)** shows a higher magnification view of upper left boxed region in **(C)**. Arrows indicate aggregates adjacent to the nucleus. **(F)** to **(K)** Confocal sections of *N. benthamiana* leaves coexpressing SGS3-YFP and TGBp1-CFP. In **(F)** to **(H)**, the yellow and cyan signals of the same plane are presented in **(F)** and **(G)**, and both signals are merged and overlaid with the bright-field image in **(H)**. Arrowheads show the region where TGBp1-CFP coaggregates with SGS3-YFP bodies. **(I)** to **(K)** show higher magnification views of the boxed regions in **(F)** to **(H)**, respectively.
(L) to **(O)** Confocal sections of *N. benthamiana* leaves coexpressing SGS3-YFP and each TGBp1-CFP mutant, $TGBp1_{AKT}$ **(L)**, $TGBp1_{E82A}$ **(M)**, $TGBp1_{P110L}$ **(N)**, and $TGBp1_{T192A}$ **(O)**. The panels show overlays of bright-field and fluorescence images.
Bars in **(A)** to **(C)**, **(F)** to **(H)**, and **(L)** to **(O)** = 25 μm; bars in **(D)** and **(E)**, **(I)** to **(K)**, and insets in **(L)** to **(O)** = 5 μm.

coexpressed with SGS3-YFP (Figure 4G; Supplemental Figure 4H). These TGBp1 aggregates were located in close proximity to the SGS3-YFP granule mass (Figures 4F to 4H; Supplemental Figures 4G to 4I). Notably, closer observation at higher magnification revealed that the TGBp1-CFP fluorescence wrapped around the SGS3-YFP granules (Figures 4I to 4K; Supplemental Figures 4J to 4L). We also found that, upon longer exposure, we could visualize TGBp1-CFP localized to plasmodesmata (Supplemental Figures 4M to 4O). These results indicated that, when coexpressed with SGS3, TGBp1 coaggregates with and enwraps SGS3/RDR6 bodies, which normally occur dispersed in the cytoplasm.

Analyses of TGBp1 Mutants

Next, we conducted a series of experiments using TGBp1 mutants. We introduced amino acid substitutions in the GKS/T motif of the NTPase/RNA helicase domain (Morozov and Solovyev, 2003) to generate $TGBp1_{AKT}$. In addition, based on the previously characterized mutation of PVX TGBp1, we constructed three other PlAMV-TGBp1 mutants; $TGBp1_{E82A}$ is predicted to retain RNA silencing suppressor activity, while $TGBp1_{P110L}$ and $TGBp1_{T192A}$ are predicted to have lost the activity (Bayne et al., 2005). Agroinfiltration-mediated transient coexpression assays of GFP and TGBp1 mutants showed that $TGBp1_{E82A}$ retained RNA silencing suppressor activity whereas $TGBp1_{AKT}$ and $TGBp1_{P110L}$ lost it (Figure 3C). In the patch expressing $TGBp1_{T192A}$, weakened GFP fluorescence was observed, indicating partial loss of RNA silencing activity in $TGBp1_{T192A}$.

We next analyzed the interaction between TGBp1 mutants and SGS3 using a BiFC assay. Coexpression of $TGBp1_{E82A}$-YFP^c or $TGBp1_{T192A}$-YFP^c with SGS3-YFP^N led to the generation of intracellular fluorescent aggregates, whereas coexpression of $TGBp1_{AKT}$-YFP^c or $TGBp1_{P110L}$-YFP^c with SGS-YFP^N failed to reconstitute YFP fluorescence (Figure 3D). These results suggested that TGBp1 mutants showing detectable RNA silencing suppressor activity can interact with SGS3, which suggests that the interaction between TGBp1 and SGS3 is involved in RNA silencing suppression by TGBp1.

We next examined the subcellular localization of TGBp1 mutants. We expressed each of the four CFP-fused TGBp1 mutants in *N. benthamiana* leaves and observed $TGBp1_{E82A}$-CFP signal localized to the nucleus and cell periphery, similar to that of wild-type TGBp1-CFP (Supplemental Figures 4Q, 4S, and 4T). By contrast, $TGBp1_{T192}$-CFP, $TGBp1_{AKT}$-CFP, and $TGBp1_{P110L}$-CFP signals lost the characteristic localization pattern of TGBp1 (Supplemental Figures 4P, 4R, and 4U to 4X). Next, we coexpressed each of the CFP-fused TGBp1 mutants and SGS3-YFP to determine whether coexpression of these proteins affects their subcellular localization. In this case, $TGBp1_{E82A}$-CFP retained the ability to aggregate SGS3 bodies like wild-type TGBp1 (Figure 4M), whereas $TGBp1_{T192}$-CFP, $TGBp1_{AKT}$-CFP, and $TGBp1_{P110L}$-CFP lost this ability (Figures 4L, 4N, and 4O). These results indicated that only $TGBp1_{E82A}$, which retains RNA silencing suppressor activity, coaggregates with SGS3 bodies, whereas $TGBp1_{T192}$, $TGBp1_{AKT}$, and $TGBp1_{P110L}$, which partially or completely lost suppressor activity, do not form such coaggregates.

TGBp1 Forms Homooligomers

Previous reports showed that PVX TGBp1 forms homooligomers (Leshchiner et al., 2008); therefore, we investigated the relationships among TGBp1 homooligomerization, suppression of RNA silencing, and coaggregation with SGS3. We first determined whether PlAMV-TGBp1 forms homooligomers. In *N. benthamiana* leaves where TGBp1 was agroinfiltrated, three distinct bands with molecular masses of ~25, 50, and 75 kD were detected (Figure 5A, lane 2), corresponding to the monomer, dimer, and trimer of TGBp1, respectively. Only TGBp1 monomers were detected in the insoluble P30 fraction, while TGBp1 oligomers as well as monomers were detected in the soluble S30 fraction (Figure 5A). These data showed that PlAMV-TGBp1, like PVX-TGBp1, forms homooligomers and they accumulate as soluble proteins in the cell.

We next examined the ability of the four TGBp1 mutants ($TGBp1_{AKT}$, $TGBp1_{E82A}$, $TGBp1_{P110L}$, and $TGBp1_{T192A}$) to form homooligomers by immunoblotting. Only $TGBp1_{E82A}$ formed oligomers, while $TGBp1_{AKT}$, $TGBp1_{P110L}$, and $TGBp1_{T192A}$ did not (Figure 5B). This result was confirmed by the quantification of each band representing the monomer (25 kD), dimer (50 kD), and trimer (75 kD) in Figure 5B (Figure 5C). Taken together, we demonstrated that only $TGBp1_{E82A}$, which retains RNA silencing suppressor activity and coaggregates with SGS3, could form homooligomers.

TGBp1 Increases Accumulation of the 2b Deletion Mutant of CMV

To examine whether TGBp1 actually suppresses SGS3/RDR6-dependent dsRNA synthesis to facilitate viral infection, we inoculated wild-type Col-0 plants, *sgs3* and *rdr6* mutants, and the TGBp1 transformants (1F and 7A) with a 2b deletion mutant of CMV (CMV-Δ2b), which induces severe symptoms and elevated levels of virus accumulation in *sgs3* and *rdr6* compared with those in wild-type Col-0 (Wang et al., 2011). Inoculation of CMV-Δ2b to *rdr6* and *sgs3* indeed caused severe symptoms (Figure 6A). RNA gel blot analysis showed that the levels of CMV-Δ2b genomic and subgenomic RNA in *rdr6* and *sgs3* plants were ~5 to 11 times higher compared with those in GUS transformants (Figure 6B). Inoculation of CMV-Δ2b to TGBp1 transformants caused even more severe symptoms than those in *rdr6* and *sgs3* mutants (Figure 6A). Accordingly, the accumulations of CMV-Δ2b RNA were ~12 to 38 times higher in TGBp1 transformants compared with those in GUS transformants (Figure 6B). These data indicated that the TGBp1 transformants showed enhanced susceptibility to CMV-Δ2b, similar to that observed in the *rdr6* and *sgs3* mutants. This suggested that TGBp1 suppresses antiviral RNA silencing by inhibiting the functions of SGS3 and RDR6.

DISCUSSION

In this study, we show that potexviral TGBp1, a well-known VSR, interferes with dsRNA synthesis by interacting with and aggregating SGS3/RDR6 bodies. So far, siRNA binding and AGO1 inactivation have been regarded as general means to suppress RNA silencing. Inhibition of dsRNA synthesis and subsequent secondary siRNA synthesis can be another candidate for the

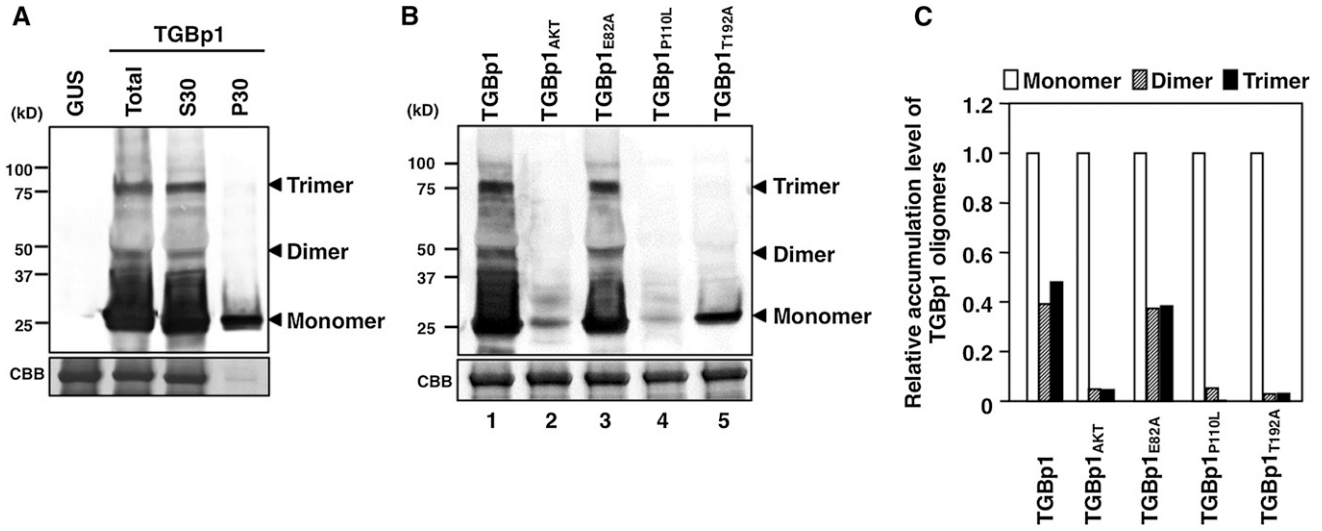

Figure 5. TGBp1 Forms Homooligomers.

(A) Immunoblot analysis of fractionated proteins extracted from *N. benthamiana* leaves transiently expressing TGBp1. Total proteins extracted from agroinfiltrated leaves at 3 d after inoculation were subjected to ultracentrifugation at 30,000*g* for 30 min to obtain the insoluble protein fraction (P30) and the soluble protein fraction (S30) and were analyzed by immunoblotting using anti-TGBp1 antibody. Coomassie Brilliant Blue (CBB) staining is shown as a loading control.

(B) Immunoblot analysis of TGBp1 mutants. Total proteins extracted from agroinfiltrated leaves were analyzed by immunoblotting using anti-TGBp1 antibody. Coomassie blue staining is shown as a loading control.

(C) Quantification of each band representing monomers (25 kD), dimers (50 kD), and trimers (75 kD) in **(B)** by ImageJ software version 1.40. The bars show accumulation levels relative to the monomer of each TGBp1 mutant.

general strategy employed by VSRs, because some VSRs have been supposed to be involved in that pathway. p2 of rice stripe tenuivirus and p6 of rice yellow stunt rhabdovirus interacted with SGS3 and RDR6, respectively (Du et al., 2011; Guo et al., 2013). V2 encoded by tomato yellow leaf curl geminivirus also interacted with and colocalized with SGS3 (Glick et al., 2008). However, in another study, V2 interacted with dsRNA to prevent SGS3 from accessing its substrate (Fukunaga and Doudna, 2009). In addition, cauliflower mosaic virus transactivator (CaMV TAV) interferes with DCL4 to perturb secondary siRNA synthesis (Shivaprasad et al., 2008). Thus, some VSRs seem to inhibit dsRNA and secondary siRNA synthesis, but biological characterization of their functions is still limited. Here, we characterized the molecular mechanism of TGBp1 to suppress dsRNA synthesis. The 5′ rapid amplification of cDNA ends, RNA gel blot analysis, and RNase protection assays presented clear evidence that TGBp1 blocks dsRNA synthesis (Figure 2). This result was supported by the biological evidence that CMV-Δ2b accumulation was elevated in TGBp1 transgenic plants, indicating that TGBp1 suppresses dsRNA synthesis to enhance viral infectivity (Figure 6). Further immunoprecipitation assays and microscopy observations revealed that TGBp1 interacts with both SGS3 and RDR6 and coaggregates and enwraps SGS3/RDR6 bodies (Figures 3, 4, and 7). These findings will advance our understanding of the molecular functions of VSRs that suppresses dsRNA synthesis in host antiviral RNA silencing to enhance viral infectivity.

We found that the TGBp1 transgenic *Arabidopsis* plants show noticeable developmental abnormalities, such as downward curling of leaf margins. To date, some VSRs have been shown to interfere with (as a side effect) endogenous RNA silencing pathways, which is probably due to sharing of common factors between antiviral and endogenous RNA silencing pathways (Kasschau et al., 2003; Chapman et al., 2004; Dunoyer et al., 2004; Zhang et al., 2006; Moissiard et al., 2007). For example, transgenic expression of CMV 2b, which inhibits AGO1 cleavage activity to block endogenous miRNA pathways, leads to developmental abnormalities similar to those of *dcl1*, *hyl1*, *se*, and *ago1* mutants defective in the miRNA pathway. Similarly, the phenotypes displayed on TGBp1 transgenic plants resembled those of tasiRNA mutants, another class of endogenous plant sRNAs (*sgs3*, *rdr6*, *dcl4*, and *ago7*) (Figure 1A). Indeed, in the TGBp1 transgenic plants, the levels of tasiRNA were significantly reduced (Figure 1C; Supplemental Table 2), and the levels of tasiRNA target mRNA increased (Figure 1D). Although previous reports have indicated that PVX-TGBp1 transformants do not exhibit any visible developmental abnormalities (Dunoyer et al., 2004), this may be due to the low level of suppressor activity of PVX TGBp1 (Senshu et al., 2009).

We showed that silencing suppression by TGBp1 is dependent not only on interaction with SGS3/RDR6 but also its homooligomerization. All TGBp1 mutants incapable of oligomerization could not aggregate SGS3/RDR6 bodies, indicating that TGBp1 oligomerization is required for the aggregation of SGS3/RDR6 bodies (Supplemental Table 3). However, $TGBp1_{T192A}$ could not form homooligomers; therefore, it could not aggregate SGS3/RDR6 bodies, but it still retained the interaction with SGS3. $TGBp1_{T192A}$ showed a partial silencing suppression activity, indicating that both interaction with SGS3 and oligomerization are required for TGBp1 to exhibit the intact silencing suppression activity.

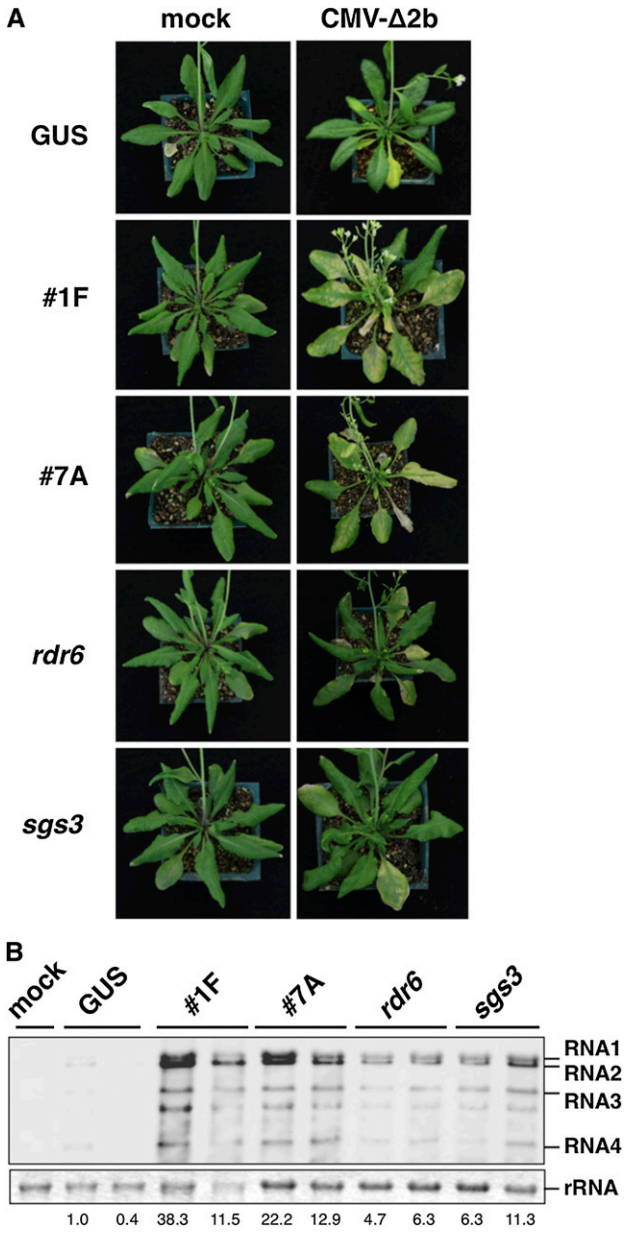

Figure 6. TGBp1 Increases the Accumulation Level of the 2b Deletion Mutant of CMV.

(A) Symptoms of *Arabidopsis* plants (GUS transformants, the TGBp1 transgenic lines 1F and 7A, and the *rdr6 and sgs3* mutants) infected with CMV-Δ2b. Plants were mechanically inoculated using sap from CMV-Δ2b–infected *N. benthamiana* leaves and photographed 3 weeks after inoculation.

(B) RNA gel blot analysis of CMV-Δ2b RNAs in the plants shown in **(A)** using a DIG-labeled RNA probe specific for the 3′ untranslated region conserved in all four CMV RNAs. rRNA was used as the loading control. The numbers below each lane show average signal intensities of RNA1, RNA2, and RNA3 relative to the GUS transformants.

Coimmunoprecipitation immunoblot assays demonstrated that TGBp1 interacts with SGS3 and RDR6. Moreover, the interaction between TGBp1 and SGS3 was confirmed using BiFC analysis. The reason that we could not detect the interaction of TGBp1 with RDR6 using the BiFC assay could be due to the low expression level of RDR6. It is possible that *Agrobacterium tumefaciens*–mediated transient expression of RDR6, a factor involved in transgene-induced RNA silencing, may lead to unexpectedly strong RNA silencing against *RDR6* itself (Vaucheret, 2006). However, both of these interactions may not necessarily be direct, since SGS3 and RDR6 are known to interact with each other (Kumakura et al., 2009).

The amplification of RNA silencing plays an important role in antiviral defense. Indeed, the accumulation of some plant viruses is markedly increased in *sgs3* and *rdr6* mutants (Garcia-Ruiz et al., 2010; Wang et al., 2011). Although increased accumulation

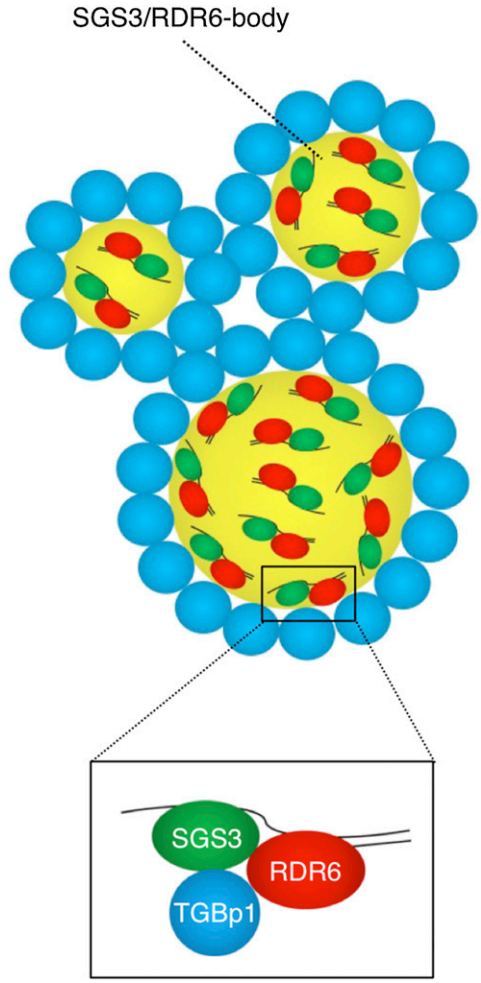

Figure 7. A Model Explaining the Mechanism of RNA Silencing Inhibition Mediated by TGBp1.

TGBp1 inhibits dsRNA synthesis by interacting with RDR6 and SGS3, which are localized to SGS3/RDR6 bodies dispersed in the cytoplasm, and by forming the aggregates with SGS3/RDR6 bodies as a result of its ability to form homooligomers.

of CMV-Δ2b is expected to generate larger amounts of dsRNA replicative intermediates, the accumulation of total vsiRNA of CMV was significantly decreased in *sgs3* and *rdr6* plants. This suggests that the vast majority of vsiRNAs accumulating in CMV-Δ2b–infected wild-type plants are secondary, not primary, vsiRNAs, which were produced by SGS3/RDR6 (Wang et al., 2011). In this study, we showed that the level of CMV-Δ2b RNA in TGBp1 transformants was significantly higher compared with that in GUS transformants (Figure 6). This revealed that TGBp1 promotes virus infection, possibly by preventing the amplification of RNA silencing against viral RNA.

Thus, we showed that both the interaction of TGBp1 and SGS3/RDR6 and the coaggregation of SGS3/RDR6 bodies by TGBp1 have important roles for the inhibition of dsRNA synthesis by TGBp1. However, we detected 5′ and 3′ cleaved products of TAS2 and TAS3 precursors in TGBp1 transformants by RLM-5′ RACE assay and RNA gel blot analysis (Figure 4B; Supplemental Figure 2). Since SGS3 has been shown to interact with 5′ and 3′ cleaved products of TAS1 and TAS2 and to stabilize them (Yoshikawa et al., 2005), detection of 5′ and 3′ cleaved RNA of TAS precursors in TGBp1 transformants may indicate that SGS3 still has a partial function to protect the 5′ and 3′ cleaved product of TAS precursor RNA from degradation in the presence of TGBp1. Therefore, TGBp1 may have some additional role(s) to inactivate components or reactions downstream from SGS3 for the inhibition of dsRNA synthesis, and the aggregation of SGS3/RDR6 bodies may facilitate these roles.

One hypothesis for TGBp1's additional function is that since TGBp1 of potexviruses contains a set of seven conserved helicase motifs and has unwinding activity on partially duplexed RNA in vitro (Kalinina et al., 2002), this RNA helicase activity of TGBp1 may be associated with the inhibition of dsRNA synthesis. It is attractive to think that TGBp1 may interact physically with and unwind the dsRNA synthesized by SGS3/RDR6 immediately after their synthesis. The unwinding of dsRNA was suggested in studies of SDE3, an RNA helicase–like protein identified as a factor required for RNA silencing (Dalmay et al., 2000, 2001). SDE3 is involved in antiviral silencing and the spread of RNA silencing by facilitating the amplification of RNA silencing by unwinding dsRNA synthesized by RDR6 and interacting with AGO1 or AGO2 to provide additional sets of aberrant RNA templates to RDR6 (Himber et al., 2003; Garcia et al., 2012), although SDE3 is not involved in the tasiRNA pathway (Vazquez et al., 2004). It will be intriguing to examine whether TGBp1 competes with the activity of SDE3.

Another scenario is that TGBp1 may inhibit RNA transfer from SGS3/RDR6 bodies. In the current model, the dsRNAs synthesized by SGS3/RDR6 are also transported from SGS3/RDR6 bodies into the nucleus (Kumakura et al., 2009; Jouannet et al., 2012). Since SDE5 encodes a putative RNA export protein required for the sense transgene–induced RNA silencing (S-RNAi) and tasiRNA pathways, but not for the inverted repeat transgene–induced RNA silencing (IR-RNAi), similar to SGS3 and RDR6 (Hernandez-Pinzon et al., 2007; Jauvion et al., 2010), SDE5 may play a role in RNA transport in conjunction with SGS3 and RDR6, although it remains unknown whether SDE5 participates in the export of RNA from the nucleus to the cytoplasm or import from the cytoplasm to the nucleus (Jauvion et al., 2010). Therefore, TGBp1 may interfere with the role of SDE5 to transport RNAs required for the amplification phase of RNA silencing.

A recent study suggested that PVX-TGBp1 interacts with AGO1 and leads to its degradation via a proteasome-dependent pathway (Chiu et al., 2010). Although we have not investigated whether PlAMV-TGBp1 interacts with AGO1, we showed that the TAS2 primary transcript was normally cleaved in the PlAMV-TGBp1 transformants (Figure 2B, lanes 3 to 5; Supplemental Figure 2), suggesting that PlAMV-TGBp1 does not significantly inhibit the slicing activity of AGO1. Moreover, unlike other VSRs that target AGO1, transgenic expression of PVX TGBp1 in plants neither induced developmental abnormalities nor exerted any noticeable effect on miRNA accumulation (Dunoyer et al., 2004; Moissiard et al., 2007). However, it is possible that TGBp1 of potexviruses targets multiple components in the antiviral RNA silencing pathway like CymRSV p19 and CMV 2b (Burgyán and Havelda, 2011), and AGO1 inactivation by PVX TGBp1 may not be sufficient to produce *ago1* phenotypes.

In support of the notion that TGBp1 may have multiple targets, we showed that the levels of CMV-Δ2b in TGBp1 transformants were much higher compared with those in the *sgs3* and *rdr6* mutants (Figure 6B). This indicates that TGBp1 may target other components of RNA silencing, such as AGO1, AGO2, DCL2, and DCL4. Moreover, miR822 is a DCL4-dependent miRNA (Rajagopalan et al., 2006). The accumulation of miR822 was significantly reduced in TGBp1 transformants compared with that in GUS transformants (Supplemental Data Set 1). Therefore, it is possible that TGBp1 has another role, to interfere with DCL4, similar to CaMV TAV (Shivaprasad et al., 2008), in addition to the inhibition of dsRNA synthesis.

In this study, we revealed that TGBp1 oligomers were detected in the soluble fraction by subcellular fractionation while the insoluble membrane-associated fraction consisted only of TGBp1 monomers (Figure 5A). This result suggested the existence of at least two distinct pools of TGBp1, one composed of homo-oligomers, likely to suppress RNA silencing in the cytoplasm, and the other predominantly consisting of monomers, likely to be involved in other aspects of viral infection, such as cell-to-cell movement through plasmodesmata (Figure 4D; Supplemental Figures 4A to 4C). This feature may be analogous to the case of the 130-kD replication protein (130K) of tomato mosaic tobamovirus (ToMV), which also functions as a VSR (Hagiwara-Komoda et al., 2008). While the membrane-associated form of 130K is involved in viral replication, the residual soluble form of 130K suppresses RNA silencing in the cytoplasm (Nishikiori et al., 2006). Since ToMV 130K has been suggested to possess optimal affinity with membrane to maintain balanced accumulation of its membrane-bound form and soluble form, TGBp1 may be properly regulated to promote efficient viral propagation.

The aggregates composed of TGBp1 and SGS3/RDR6 bodies observed in this study closely resemble amorphous inclusion bodies, induced by PVX infection and localized next to the nucleus (Figures 4F to 4K; Tilsner et al., 2012). The inclusion body was reported to include PVX TGBp1 aggregates surrounded by recruited host actin, endoplasmic reticulum, and Golgi apparatus. Moreover, the inclusion body included viral replicase and non-encapsidated viral RNA incorporated within TGBp2/3-containing endoplasmic reticulum–derived granular vesicles, suggesting that

the inclusion body is a highly organized virus replication "factory." Since characteristics of the inclusion body, such as its size and shape, agree with those of PlAMV-TGBp1 aggregates with SGS3/RDR6 bodies, inclusion bodies formed within infected cells by potexviruses may include SGS3/RDR6 as well as viral RNA, replicase, TGBps, and other host components required for viral replication and movement.

The inhibition of dsRNA synthesis observed in this study might be a general strategy of RNA silencing suppression. TGBp1 suppresses S-RNAi but not IR-RNAi (Senshu et al., 2009). This is consistent with the finding that TGBp1 inactivates SGS3/RDR6-mediated dsRNA synthesis because SGS3 and RDR6 are only involved in S-RNAi, but AGO1 and DCL4 are involved in both S-RNAi and IR-RNAi. Several examples of VSRs, such as p69 encoded by turnip yellow mosaic tymovirus and NSs encoded by tomato spotted wilt tospovirus, suppress S-RNAi but not IR-RNAi, suggesting that these VSRs may target SGS3 and/or RDR6 (Takeda et al., 2002; Chen et al., 2004). Such suppression of SGS3/RDR6-mediated dsRNA synthesis resulting in the production of secondary siRNAs may be beneficial for plant virus infection.

Furthermore, amplification of RNA silencing by RDR6 has been implicated in the spread of an RNA silencing signal (Schwach et al., 2005). This signal is supposed to prime the antiviral RNA silencing in surrounding naive cells ahead of the viral infection front. Hence, the amplification of RNA silencing by RDR6 is also important in terms of inhibiting virus movement, suggesting that inhibition of this process may have a significant beneficial effect on plant viruses. Therefore, VSRs that prevent the systemic spread of RNA silencing, such as TGBp1 of potato carlavirus M, p50 of apple chlorotic leaf spot trichovirus, and the coat protein of citrus tristeza closterovirus, may also inhibit the function of SGS3/RDR6 (Lu et al., 2004; Yaegashi et al., 2007; Senshu et al., 2011). Future studies will make it clear whether these VSRs actually suppress the activities of SGS3 and/or RDR6, thereby inhibiting the amplification of RNA silencing, to facilitate the escape of plant viruses from secondary siRNAs in both replicating and newly entered cells.

Targeting of SGS3/RDR6 may have an additional beneficial effect on plant viruses, namely, very mild developmental defects in host plants (Figure 1A). In contrast, VSRs targeting sRNAs or AGO1 induce severe developmental defects, similar to those observed in the *ago1* mutant (Figure 1A; Chapman et al., 2004; Dunoyer et al., 2004; Zhang et al., 2006). Because viruses are obligate parasites and rely almost entirely on the host cell machinery, severe developmental perturbations by a VSR may not be advantageous to the virus. In support of this hypothesis, a large number of plant viruses infect their host plants latently or with very mild symptoms. Taken together, targeting of SGS3/RDR6, which plays an important role in antiviral defense but has relatively few effects on plant development, could be highly advantageous for viruses.

METHODS

Plant Materials

Seeds of *Arabidopsis thaliana* mutants *sgs3-11* (CS24289), *rdr6-11* (CS24285), *dcl4-2e* (CS6954), *zip-1* (which has a defect in AGO7) (CS24281), and *dcl1-9* (CS3828) were provided by the ABRC. *Arabidopsis* and *Nicotiana benthamiana* plants were grown in growth chambers under 16-h-light/8-h-dark conditions at 23 and 25°C, respectively.

Plasmid Construction

All primers used in this study are listed in Supplemental Table 4. pCAMBIA1301-PlAMV-TGBp1, a binary vector expressing PlAMV-TGBp1, was described previously (Senshu et al., 2009). To generate binary vectors expressing TGBp1 mutants, we introduced mutations into pCAMBIA1301-PlAMV-TGBp1 by performing recombinant PCR using sets of two partially complementary primers: PlTGBp1AKT-F and PlTGBp1AKT-R, PlTGBp1E92A-F and PlTGBp1E92A-R, PlTGBp1P110L-F and PlTGBp1P110L-R, and PlTGBp1T192A-F and PlTGBp1T192A-R for CAMBIA1301-PlAMV-TGBp1$_{AKT}$, -TGBp1$_{E82A}$, -TGBp1$_{P110L}$, and -TGBp1$_{T192A}$, respectively.

To construct epitope-tagged expression vectors, we used LR Clonase (Invitrogen) reaction-mediated recombination into pEarleyGate vectors (Earley et al., 2006). The GUS fragment was amplified from pCAMBIA1301 using the primers ENTA-GUS-F and ENTA-GUS-R. PlAMV-TGBp1 and derivatives were amplified from the pCAMBIA1301-based TGBp1 expression vectors described above using primers ENTA-TGBp1-F and ENTA-TGBp1-R. SGS3, RDR6, and PDLP cDNA was amplified from *Arabidopsis* Col-0 total RNA using the primers ENTA-SGS3-F and ENTA-SGS3-R, ENTA-RDR6-F and ENTA-RDR6-R, and ENTA-PDLP-F and ENTA-PDLP-R, respectively. The PCR-amplified fragments were cloned into the entry vector pENTA (Himeno et al., 2010) to generate pENTA-GUS, -TGBp1, -TGBp1$_{AKT}$, -TGBp1$_{E82A}$, -TGBp1$_{P110L}$, -TGBp1$_{T192A}$, -SGS3, -RDR6, and -PDLP. pENTA-GUS, -TGBp1, -SGS3, and -RDR6 were recombined using the LR Clonase reaction into pEarleyGate202 to generate the binary vectors pEarley-GUS-FLAG, -TGBp1-FLAG, -SGS3-FLAG, and -RDR6-FLAG, respectively. Similarly, pENTR-GUS, -TGBp1, -SGS3, and -RDR6 were recombined into pEarleyGateC3myc, a pEarleyGate-based vector modified to express triple c-myc–tagged proteins, to generate pEarley-GUS-myc, -TGBp1-myc, -SGS3-myc, and -RDR6-myc, respectively.

To construct vectors for fluorescence microscopy, we also used LR Clonase reaction-based recombination. pENTA-TGBp1 and -SGS3 were recombined into pEarleyGateCBiFCN, a pEarleyGate-based vector modified to express proteins fused to the N-terminal half of YFP at their C terminus, to generate pEarley-TGBp1-YFPN and -SGS3-YFPN, respectively. pENTA-TGBp1, -TGBp1$_{AKT}$, -TGBp1$_{E82A}$, -TGBp1$_{P110L}$, -TGBp1$_{T192A}$, -SGS3, and -RDR6 were recombined into pEarleyGateCBiFCC, a vector modified to express proteins fused to the C-terminal half of YFP at their C terminus, to generate pEarley-TGBp1-YFPC, -TGBp1$_{AKT}$-YFPC, -TGBp1$_{E82A}$-YFPC, -TGBp1$_{P110L}$-YFPC, -TGBp1$_{T192A}$-YFPC, -SGS3-YFPC, and -RDR6-YFPC, respectively. pENTA-TGBp1, -TGBp1$_{AKT}$, -TGBp1$_{E82A}$, -TGBp1$_{P110L}$, and -TGBp1$_{T192A}$ were recombined into pEarleyGate102 (Earley et al., 2006) to generate pEarley-TGBp1-CFP, -TGBp1$_{AKT}$-CFP, -TGBp1$_{E82A}$-CFP, -TGBp1$_{P110L}$-CFP, and -TGBp1$_{T192A}$-CFP, respectively. pENTA-SGS3, -RDR6, and -PDLP were recombined into pEarleyGate101 to generate pEarley-SGS3-YFP, -RDR6-YFP, and -PDLP-YFP, respectively.

To generate CMV-Δ2b, infectious full-length cDNA clones of the CMV-Y strain under the control of the 35S promoter sequences were modified as described previously (Wang et al., 2011).

Plant Transformation and Agroinfiltration

Arabidopsis Col-0 plants were transformed with *Agrobacterium tumefaciens* EHA105 carrying pCAMBIA1301 and pCAMBIA1301-PlAMV-TGBp1 to generate GUS and TGBp1 transformants, respectively, using a floral dip method as described previously (Yamaji et al., 2012). Agroinfiltration was performed as described elsewhere (Senshu et al., 2009).

RNA Isolation and Detection

RNA isolation and RNA gel blot analysis of sRNAs and mRNAs were performed as described previously (Senshu et al., 2009). Digoxigenin (DIG)-labeled RNA probes corresponding to nucleotides 180 to 767 of TAS2 (At2g39680) and nucleotides 58 to 863 of TAS3 (At3g17185) were

used to detect TAS2 tasiRNA and TAS3 tasiRNA, respectively. The sequences of DIG-labeled cDNA probes to detect miR173 and miR171 were as follows: miR173, 5′-GTGATTTCTCTCTGCAAGCGAA-3′; and miR171, 5′-GATATTGGCGCGGCTCAATCA-3′. The probe for TAS2 tasiRNA was also used to detect TAS2 precursor complementary RNA. A DIG-labeled RNA probe corresponding to the 3′ terminal 240 nucleotides of CMV RNA2 was used to detect the four CMV RNAs. The primary TAS2 transcript and its cleavage products were detected from total RNAs of flowers using a DIG-labeled RNA probe corresponding to nucleotides 128 to 934 of TAS2 as described previously (Yoshikawa et al., 2013).

Quantitative real-time PCR was performed as described previously (Komatsu et al., 2010). The primers used to detect *PPR* (At1g63130), *ARF3* (At2g33860), and *ACTIN2* (At3g18780) mRNAs are listed in Supplemental Table 4.

RLM-5′ RACE and RNase Protection Assay

The 3′ cleavage products of the primary TAS transcripts were detected by RLM-5′ RACE using the GeneRacer kit (Invitrogen) following the manufacturer's instructions. Total RNA (5 μg) from *Arabidopsis* plants treated with DNase I was ligated to an RNA oligo adaptor using T4 RNA ligase and reverse-transcribed using oligo(dT) primers to synthesize cDNA. The resultant cDNA pool was used as a template for PCR using GeneRacer 5′ primer and TAS2-767R or TAS3-931R and was again PCR-amplified using GeneRacer 5′ nested primer and TAS2-725R or TAS3-910R primer (Supplemental Table 4). Amplified fragments were electrophoresed on a native 4% polyacrylamide gel and stained with ethidium bromide.

The dsRNAs of TAS2 and TAS3 precursor RNAs were analyzed using the RNase protection assay. Total RNA (5 μg) from *Arabidopsis* plants treated with DNase I was incubated with appropriate concentrations of RNase ONE Ribonuclease (Promega) for 1 h at 37°C. RNase-treated RNA was reverse-transcribed with random primer (N)9 and amplified by PCR with primers TAS2-450F and TAS2-570R for TAS2 and TAS3-704F and TAS3-841R for TAS3 (Supplemental Table 4). Amplified fragments were electrophoresed on a 3% agarose gel and stained with ethidium bromide.

Immunoblot Analysis and Immunoprecipitation

Protein extraction and immunoblot analysis were performed as described previously (Senshu et al., 2009). To prepare antibody against TGBp1, hexahistidine-tagged TGBp1 was expressed in *Escherichia coli* and purified as described previously (Yamaji et al., 2006). Polyclonal antibody against TGBp1 was raised in a rabbit using the purified protein as antigen.

For immunoprecipitation, 6 mL of total proteins was mixed with 150 μL of anti-FLAG M2 affinity gel (50% suspension; Sigma-Aldrich). After an overnight incubation, the resin was washed 10 times with PBS containing 0.05% Tween 20 and eluted in 750 μL of PBS containing 0.05% Tween 20 and 150 μg/mL 3× FLAG peptide (Sigma-Aldrich). Mouse monoclonal antibody to the FLAG peptide tag (clone M2) and rabbit polyclonal anti–c-myc antibody were obtained from Sigma-Aldrich and Cell Signaling Technology, respectively.

Fluorescence Microscopy

Confocal laser scanning microscopy analysis to detect CFP and YFP was performed as described previously (Senshu et al., 2011). For the BiFC assay, *Agrobacterium tumefaciens* culture with a binary vector expressing YFP^N-tagged protein and a vector expressing YFP^C-tagged protein was infiltrated into *N. benthamiana* leaves. Leaves were analyzed with confocal laser scanning microscopy to observe YFP fluorescence.

Construction of sRNA Libraries and Deep Sequencing

Construction of sRNA libraries and deep sequencing were performed according to the Illumina version 1.5 preparation kit protocol. Briefly, sRNAs (18 to 30 nucleotides) were purified from 5 μg of total RNA using PAGE. RNA adaptors were then ligated to the sRNAs followed by reverse transcription into cDNA. These cDNAs were amplified by 12 cycles of PCR and subjected to Illumina sequencing.

The sRNA reads were generated from Illumina Genome Analyzer IIx analysis using the Illumina Sequencing Kit version 4. After removing the adaptor sequences, the sequence data were preprocessed to remove low-quality reads including reads of <17 nucleotides and contaminating sequences formed by adaptor–adaptor ligation. The quality-filtered reads were aligned to the *Arabidopsis* genome allowing one mismatch using Bowtie software (http://bowtie-bio.sourceforge.net/index.shtml), followed by trimming of the last base at the 3′ end of unmapped reads and secondary alignment using the same parameters. This procedure was repeated until the length of unmapped reads was 17 nucleotides. Only reads that aligned to at most 29 positions in the genome were used in the following procedure. The mapped sRNAs were annotated with reference to miRBase (version 16; http://www.mirbase.org) for miRNA sequences and Ensembl Plants (http://plants.ensembl.org/index.html) for rRNA, tRNA, small nuclear RNA, small nucleolar RNA, and miscellaneous RNA sequences. All read counts were normalized to adjust for differences in library size and coverage to reads per kilobase of the exon model per million mapped reads (RPKM) according to the total read count in each library.

Accession Numbers

sRNA sequence data sets were deposited at the DNA Database of Japan (http://www.ddbj.nig.ac.jp/index-e.html) under accession number DRA001183.

Supplemental Data

The following materials are available in the online version of this article.

Supplemental Figure 1. Size Distribution of *Arabidopsis* sRNAs in the GUS and the TGBp1 Transformants.

Supplemental Figure 2. RNA Gel Blot Analysis to Detect the Primary TAS2 Transcript and Its Cleavage Products.

Supplemental Figure 3. Confocal Laser Scanning Microscopy Observation of RDR6.

Supplemental Figure 4. Subcellular Localizations of SGS3, TGBp1, and TGBp1 Mutants.

Supplemental Table 1. RPKM Value of sRNA Reads Mapped to the *Arabidopsis* Genome.

Supplemental Table 2. Comparison of RPKM Values of tasiRNAs from the GUS and TGBp1 Transformant sRNA Libraries.

Supplemental Table 3. Characteristics of TGBp1 Mutants Used in This Study.

Supplemental Table 4. Primers Used in This Study.

Supplemental Data Set 1. Comparison of RPKM Value of Known miRNAs from the GUS and TGBp1 Transformant sRNA Libraries.

ACKNOWLEDGMENTS

We thank Masashi Suzuki at The University of Tokyo for providing the infectious CMV cDNA clone. We also thank for Manabu Yoshikawa for technical advice for the RNA gel blotting of TAS precursor RNAs. This work was supported by the Program for the Promotion of Basic Research Activities for Innovative Bioscience and by Grants-in-Aid for Scientific Research from the Japan Society for the Promotion of Science.

AUTHOR CONTRIBUTIONS

Y.O., H.S., M.H., O.N., K.K., Y.Y., and S.N. designed the research. Y.O., H.S., M.H., Y.N., N.M., T.Y., and K.M. performed the research. Y.O., H.S., M.H., K.O., Y.Y., and S.N. analyzed the data. Y.O., O.N., K.K., Y.Y., and S.N. wrote the article.

Received November 7, 2013; revised April 23, 2014; accepted May 9, 2014; published May 30, 2014.

REFERENCES

Adenot, X., Elmayan, T., Lauressergues, D., Boutet, S., Bouché, N., Gasciolli, V., and Vaucheret, H. (2006). DRB4-dependent TAS3 trans-acting siRNAs control leaf morphology through AGO7. Curr. Biol. **16:** 927–932.

Allen, E., and Howell, M.D. (2010). miRNAs in the biogenesis of trans-acting siRNAs in higher plants. Semin. Cell Dev. Biol. **21:** 798–804.

Allen, E., Xie, Z., Gustafson, A.M., and Carrington, J.C. (2005). MicroRNA-directed phasing during trans-acting siRNA biogenesis in plants. Cell **121:** 207–221.

Amari, K., Lerich, A., Schmitt-Keichinger, C., Dolja, V.V., and Ritzenthaler, C. (2011). Tubule-guided cell-to-cell movement of a plant virus requires class XI myosin motors. PLoS Pathog. **7:** e1002327.

Azevedo, J., Garcia, D., Pontier, D., Ohnesorge, S., Yu, A., Garcia, S., Braun, L., Bergdoll, M., Hakimi, M.A., Lagrange, T., and Voinnet, O. (2010). Argonaute quenching and global changes in Dicer homeostasis caused by a pathogen-encoded GW repeat protein. Genes Dev. **24:** 904–915.

Bartel, D.P. (2004). MicroRNAs: Genomics, biogenesis, mechanism, and function. Cell **116:** 281–297.

Baumberger, N., and Baulcombe, D.C. (2005). Arabidopsis ARGONAUTE1 is an RNA Slicer that selectively recruits microRNAs and short interfering RNAs. Proc. Natl. Acad. Sci. USA **102:** 11928–11933.

Baumberger, N., Tsai, C.H., Lie, M., Havecker, E., and Baulcombe, D.C. (2007). The Polerovirus silencing suppressor P0 targets ARGONAUTE proteins for degradation. Curr. Biol. **17:** 1609–1614.

Bayne, E.H., Rakitina, D.V., Morozov, S.Y., and Baulcombe, D.C. (2005). Cell-to-cell movement of potato potexvirus X is dependent on suppression of RNA silencing. Plant J. **44:** 471–482.

Blevins, T., Rajeswaran, R., Shivaprasad, P.V., Beknazariants, D., Si-Ammour, A., Park, H.S., Vazquez, F., Robertson, D., Meins, F., Jr., Hohn, T., and Pooggin, M.M. (2006). Four plant Dicers mediate viral small RNA biogenesis and DNA virus induced silencing. Nucleic Acids Res. **34:** 6233–6246.

Bortolamiol, D., Pazhouhandeh, M., Marrocco, K., Genschik, P., and Ziegler-Graff, V. (2007). The Polerovirus F box protein P0 targets ARGONAUTE1 to suppress RNA silencing. Curr. Biol. **17:** 1615–1621.

Brigneti, G., Voinnet, O., Li, W.X., Ji, L.H., Ding, S.W., and Baulcombe, D.C. (1998). Viral pathogenicity determinants are suppressors of transgene silencing in *Nicotiana benthamiana*. EMBO J. **17:** 6739–6746.

Burgyán, J., and Havelda, Z. (2011). Viral suppressors of RNA silencing. Trends Plant Sci. **16:** 265–272.

Chapman, E.J., Prokhnevsky, A.I., Gopinath, K., Dolja, V.V., and Carrington, J.C. (2004). Viral RNA silencing suppressors inhibit the microRNA pathway at an intermediate step. Genes Dev. **18:** 1179–1186.

Chen, J., Li, W.X., Xie, D., Peng, J.R., and Ding, S.W. (2004). Viral virulence protein suppresses RNA silencing-mediated defense but upregulates the role of microRNA in host gene expression. Plant Cell **16:** 1302–1313.

Chiu, M.H., Chen, I.H., Baulcombe, D.C., and Tsai, C.H. (2010). The silencing suppressor P25 of Potato virus X interacts with Argonaute1 and mediates its degradation through the proteasome pathway. Mol. Plant Pathol. **11:** 641–649.

Dalmay, T., Hamilton, A., Rudd, S., Angell, S., and Baulcombe, D.C. (2000). An RNA-dependent RNA polymerase gene in Arabidopsis is required for posttranscriptional gene silencing mediated by a transgene but not by a virus. Cell **101:** 543–553.

Dalmay, T., Horsefield, R., Braunstein, T.H., and Baulcombe, D.C. (2001). SDE3 encodes an RNA helicase required for post-transcriptional gene silencing in Arabidopsis. EMBO J. **20:** 2069–2078.

Deleris, A., Gallego-Bartolome, J., Bao, J., Kasschau, K.D., Carrington, J.C., and Voinnet, O. (2006). Hierarchical action and inhibition of plant Dicer-like proteins in antiviral defense. Science **313:** 68–71.

Diaz-Pendon, J.A., Li, F., Li, W.X., and Ding, S.W. (2007). Suppression of antiviral silencing by cucumber mosaic virus 2b protein in *Arabidopsis* is associated with drastically reduced accumulation of three classes of viral small interfering RNAs. Plant Cell **19:** 2053–2063.

Ding, S.W., and Voinnet, O. (2007). Antiviral immunity directed by small RNAs. Cell **130:** 413–426.

Du, Z., Xiao, D., Wu, J., Jia, D., Yuan, Z., Liu, Y., Hu, L., Han, Z., Wei, T., Lin, Q., Wu, Z., and Xie, L. (2011). p2 of rice stripe virus (RSV) interacts with OsSGS3 and is a silencing suppressor. Mol. Plant Pathol. **12:** 808–814.

Dunoyer, P., Lecellier, C.H., Parizotto, E.A., Himber, C., and Voinnet, O. (2004). Probing the microRNA and small interfering RNA pathways with virus-encoded suppressors of RNA silencing. Plant Cell **16:** 1235–1250.

Earley, K.W., Haag, J.R., Pontes, O., Opper, K., Juehne, T., Song, K., and Pikaard, C.S. (2006). Gateway-compatible vectors for plant functional genomics and proteomics. Plant J. **45:** 616–629.

Elmayan, T., Adenot, X., Gissot, L., Lauressergues, D., Gy, I., and Vaucheret, H. (2009). A neomorphic *sgs3* allele stabilizing miRNA cleavage products reveals that SGS3 acts as a homodimer. FEBS J. **276:** 835–844.

Fukunaga, R., and Doudna, J.A. (2009). dsRNA with 5′ overhangs contributes to endogenous and antiviral RNA silencing pathways in plants. EMBO J. **28:** 545–555.

Garcia, D., Garcia, S., Pontier, D., Marchais, A., Renou, J.P., Lagrange, T., and Voinnet, O. (2012). Ago hook and RNA helicase motifs underpin dual roles for SDE3 in antiviral defense and silencing of nonconserved intergenic regions. Mol. Cell **48:** 109–120.

Garcia-Ruiz, H., Takeda, A., Chapman, E.J., Sullivan, C.M., Fahlgren, N., Brempelis, K.J., and Carrington, J.C. (2010). Arabidopsis RNA-dependent RNA polymerases and Dicer-like proteins in antiviral defense and small interfering RNA biogenesis during turnip mosaic virus infection. Plant Cell **22:** 481–496.

Giner, A., Lakatos, L., García-Chapa, M., López-Moya, J.J., and Burgyán, J. (2010). Viral protein inhibits RISC activity by argonaute binding through conserved WG/GW motifs. PLoS Pathog. **6:** e1000996.

Glick, E., Zrachya, A., Levy, Y., Mett, A., Gidoni, D., Belausov, E., Citovsky, V., and Gafni, Y. (2008). Interaction with host SGS3 is required for suppression of RNA silencing by tomato yellow leaf curl virus V2 protein. Proc. Natl. Acad. Sci. USA **105:** 157–161.

Guo, H., Song, X., Xie, C., Huo, Y., Zhang, F., Chen, X., Geng, Y., and Fang, R. (2013). Rice yellow stunt rhabdovirus protein 6 suppresses systemic RNA silencing by blocking RDR6-mediated secondary siRNA synthesis. Mol. Plant Microbe Interact. **26:** 927–936.

Hagiwara-Komoda, Y., Hirai, K., Mochizuki, A., Nishiguchi, M., Meshi, T., and Ishikawa, M. (2008). Overexpression of a host factor TOM1 inhibits tomato mosaic virus propagation and suppression of RNA silencing. Virology **376:** 132–139.

Hernandez-Pinzon, I., Yelina, N.E., Schwach, F., Studholme, D.J., Baulcombe, D., and Dalmay, T. (2007). SDE5, the putative homologue of a human mRNA export factor, is required for transgene silencing and accumulation of trans-acting endogenous siRNA. Plant J. **50:** 140–148.

Himber, C., Dunoyer, P., Moissiard, G., Ritzenthaler, C., and Voinnet, O. (2003). Transitivity-dependent and -independent cell-to-cell movement of RNA silencing. EMBO J. **22:** 4523–4533.

Himeno, M., Maejima, K., Komatsu, K., Ozeki, J., Hashimoto, M., Kagiwada, S., Yamaji, Y., and Namba, S. (2010). Significantly low level of small RNA accumulation derived from an encapsidated mycovirus with dsRNA genome. Virology **396:** 69–75.

Jauvion, V., Elmayan, T., and Vaucheret, H. (2010). The conserved RNA trafficking proteins HPR1 and TEX1 are involved in the production of endogenous and exogenous small interfering RNA in *Arabidopsis*. Plant Cell **22:** 2697–2709.

Jouannet, V., Moreno, A.B., Elmayan, T., Vaucheret, H., Crespi, M.D., and Maizel, A. (2012). Cytoplasmic Arabidopsis AGO7 accumulates in membrane-associated siRNA bodies and is required for ta-siRNA biogenesis. EMBO J. **31:** 1704–1713.

Kalantidis, K., Schumacher, H.T., Alexiadis, T., and Helm, J.M. (2008). RNA silencing movement in plants. Biol. Cell **100:** 13–26.

Kalinina, N.O., Rakitina, D.V., Solovyev, A.G., Schiemann, J., and Morozov, S.Y. (2002). RNA helicase activity of the plant virus movement proteins encoded by the first gene of the triple gene block. Virology **296:** 321–329.

Kasschau, K.D., Xie, Z., Allen, E., Llave, C., Chapman, E.J., Krizan, K.A., and Carrington, J.C. (2003). P1/HC-Pro, a viral suppressor of RNA silencing, interferes with Arabidopsis development and miRNA function. Dev. Cell **4:** 205–217.

Komatsu, K., Hashimoto, M., Ozeki, J., Yamaji, Y., Maejima, K., Senshu, H., Himeno, M., Okano, Y., Kagiwada, S., and Namba, S. (2010). Viral-induced systemic necrosis in plants involves both programmed cell death and the inhibition of viral multiplication, which are regulated by independent pathways. Mol. Plant Microbe Interact. **23:** 283–293.

Kumakura, N., Takeda, A., Fujioka, Y., Motose, H., Takano, R., and Watanabe, Y. (2009). SGS3 and RDR6 interact and colocalize in cytoplasmic SGS3/RDR6-bodies. FEBS Lett. **583:** 1261–1266.

Lakatos, L., Csorba, T., Pantaleo, V., Chapman, E.J., Carrington, J.C., Liu, Y.P., Dolja, V.V., Calvino, L.F., López-Moya, J.J., and Burgyán, J. (2006). Small RNA binding is a common strategy to suppress RNA silencing by several viral suppressors. EMBO J. **25:** 2768–2780.

Leshchiner, A.D., Minina, E.A., Rakitina, D.V., Vishnichenko, V.K., Solovyev, A.G., Morozov, S.Y., and Kalinina, N.O. (2008). Oligomerization of the potato virus X 25-kD movement protein. Biochemistry (Mosc.) **73:** 50–55.

Liu, X., and Gorovsky, M.A. (1993). Mapping the 5′ and 3′ ends of Tetrahymena thermophila mRNAs using RNA ligase mediated amplification of cDNA ends (RLM-RACE). Nucleic Acids Res. **21:** 4954–4960.

Lu, R., Folimonov, A., Shintaku, M., Li, W.X., Falk, B.W., Dawson, W.O., and Ding, S.W. (2004). Three distinct suppressors of RNA silencing encoded by a 20-kb viral RNA genome. Proc. Natl. Acad. Sci. USA **101:** 15742–15747.

Mérai, Z., Kerényi, Z., Kertész, S., Magna, M., Lakatos, L., and Silhavy, D. (2006). Double-stranded RNA binding may be a general plant RNA viral strategy to suppress RNA silencing. J. Virol. **80:** 5747–5756.

Moissiard, G., Parizotto, E.A., Himber, C., and Voinnet, O. (2007). Transitivity in Arabidopsis can be primed, requires the redundant action of the antiviral Dicer-like 4 and Dicer-like 2, and is compromised by viral-encoded suppressor proteins. RNA **13:** 1268–1278.

Montgomery, T.A., Howell, M.D., Cuperus, J.T., Li, D., Hansen, J.E., Alexander, A.L., Chapman, E.J., Fahlgren, N., Allen, E., and Carrington, J.C. (2008a). Specificity of ARGONAUTE7-miR390 interaction and dual functionality in TAS3 trans-acting siRNA formation. Cell **133:** 128–141.

Montgomery, T.A., Yoo, S.J., Fahlgren, N., Gilbert, S.D., Howell, M.D., Sullivan, C.M., Alexander, A., Nguyen, G., Allen, E., Ahn, J. H., and Carrington, J.C. (2008b). AGO1-miR173 complex initiates phased siRNA formation in plants. Proc. Natl. Acad. Sci. USA **105:** 20055–20062.

Morel, J.B., Godon, C., Mourrain, P., Béclin, C., Boutet, S., Feuerbach, F., Proux, F., and Vaucheret, H. (2002). Fertile hypomorphic *ARGONAUTE* (*ago1*) mutants impaired in post-transcriptional gene silencing and virus resistance. Plant Cell **14:** 629–639.

Morozov, S.Y., and Solovyev, A.G. (2003). Triple gene block: Modular design of a multifunctional machine for plant virus movement. J. Gen. Virol. **84:** 1351–1366.

Nakazawa, Y., Hiraguri, A., Moriyama, H., and Fukuhara, T. (2007). The dsRNA-binding protein DRB4 interacts with the Dicer-like protein DCL4 in vivo and functions in the trans-acting siRNA pathway. Plant Mol. Biol. **63:** 777–785.

Nishikiori, M., Dohi, K., Mori, M., Meshi, T., Naito, S., and Ishikawa, M. (2006). Membrane-bound tomato mosaic virus replication proteins participate in RNA synthesis and are associated with host proteins in a pattern distinct from those that are not membrane bound. J. Virol. **80:** 8459–8468.

Peragine, A., Yoshikawa, M., Wu, G., Albrecht, H.L., and Poethig, R.S. (2004). SGS3 and SGS2/SDE1/RDR6 are required for juvenile development and the production of trans-acting siRNAs in Arabidopsis. Genes Dev. **18:** 2368–2379.

Rajagopalan, R., Vaucheret, H., Trejo, J., and Bartel, D.P. (2006). A diverse and evolutionarily fluid set of microRNAs in *Arabidopsis thaliana*. Genes Dev. **20:** 3407–3425.

Schwach, F., Vaistij, F.E., Jones, L., and Baulcombe, D.C. (2005). An RNA-dependent RNA polymerase prevents meristem invasion by potato virus X and is required for the activity but not the production of a systemic silencing signal. Plant Physiol. **138:** 1842–1852.

Senshu, H., Ozeki, J., Komatsu, K., Hashimoto, M., Hatada, K., Aoyama, M., Kagiwada, S., Yamaji, Y., and Namba, S. (2009). Variability in the level of RNA silencing suppression caused by triple gene block protein 1 (TGBp1) from various potexviruses during infection. J. Gen. Virol. **90:** 1014–1024.

Senshu, H., Yamaji, Y., Minato, N., Shiraishi, T., Maejima, K., Hashimoto, M., Miura, C., Neriya, Y., and Namba, S. (2011). A dual strategy for the suppression of host antiviral silencing: Two distinct suppressors for viral replication and viral movement encoded by potato virus M. J. Virol. **85:** 10269–10278.

Shivaprasad, P.V., Rajeswaran, R., Blevins, T., Schoelz, J., Meins, F., Jr., Hohn, T., and Pooggin, M.M. (2008). The CaMV transactivator/viroplasmin interferes with RDR6-dependent trans-acting and secondary siRNA pathways in Arabidopsis. Nucleic Acids Res. **36:** 5896–5909.

Takeda, A., Sugiyama, K., Nagano, H., Mori, M., Kaido, M., Mise, K., Tsuda, S., and Okuno, T. (2002). Identification of a novel RNA silencing suppressor, NSs protein of Tomato spotted wilt virus. FEBS Lett. **532:** 75–79.

Tilsner, J., Linnik, O., Wright, K.M., Bell, K., Roberts, A.G., Lacomme, C., Santa Cruz, S., and Oparka, K.J. (2012). The TGB1 movement protein of *Potato virus X* reorganizes actin and endomembranes into the X-body, a viral replication factory. Plant Physiol. **158:** 1359–1370.

Várallyay, E., Válóczi, A., Agyi, A., Burgyán, J., and Havelda, Z. (2010). Plant virus-mediated induction of miR168 is associated with repression of ARGONAUTE1 accumulation. EMBO J. **29:** 3507–3519.

Vargason, J.M., Szittya, G., Burgyán, J., and Hall, T.M. (2003). Size selective recognition of siRNA by an RNA silencing suppressor. Cell **115:** 799–811.

Vaucheret, H. (2006). Post-transcriptional small RNA pathways in plants: Mechanisms and regulations. Genes Dev. **20:** 759–771.

Vazquez, F., Vaucheret, H., Rajagopalan, R., Lepers, C., Gasciolli, V., Mallory, A.C., Hilbert, J.L., Bartel, D.P., and Crété, P. (2004). Endogenous trans-acting siRNAs regulate the accumulation of Arabidopsis mRNAs. Mol. Cell **16:** 69–79.

Voinnet, O., and Baulcombe, D.C. (1997). Systemic signalling in gene silencing. Nature **389:** 553.

Voinnet, O., Lederer, C., and Baulcombe, D.C. (2000). A viral movement protein prevents spread of the gene silencing signal in *Nicotiana benthamiana*. Cell **103:** 157–167.

Voinnet, O., Pinto, Y.M., and Baulcombe, D.C. (1999). Suppression of gene silencing: A general strategy used by diverse DNA and RNA viruses of plants. Proc. Natl. Acad. Sci. USA **96:** 14147–14152.

Voinnet, O., Vain, P., Angell, S., and Baulcombe, D.C. (1998). Systemic spread of sequence-specific transgene RNA degradation in plants is initiated by localized introduction of ectopic promoterless DNA. Cell **95:** 177–187.

Wang, X.B., Jovel, J., Udomporn, P., Wang, Y., Wu, Q., Li, W.X., Gasciolli, V., Vaucheret, H., and Ding, S.W. (2011). The 21-nucleotide, but not 22-nucleotide, viral secondary small interfering RNAs direct potent antiviral defense by two cooperative argonautes in *Arabidopsis thaliana*. Plant Cell **23:** 1625–1638.

Xie, Z., Allen, E., Wilken, A., and Carrington, J.C. (2005). DICER-LIKE 4 functions in trans-acting small interfering RNA biogenesis and vegetative phase change in *Arabidopsis thaliana*. Proc. Natl. Acad. Sci. USA **102:** 12984–12989.

Yaegashi, H., Takahashi, T., Isogai, M., Kobori, T., Ohki, S., and Yoshikawa, N. (2007). Apple chlorotic leaf spot virus 50 kDa movement protein acts as a suppressor of systemic silencing without interfering with local silencing in *Nicotiana benthamiana*. J. Gen. Virol. **88:** 316–324.

Yamaji, Y., Kobayashi, T., Hamada, K., Sakurai, K., Yoshii, A., Suzuki, M., Namba, S., and Hibi, T. (2006). In vivo interaction between Tobacco mosaic virus RNA-dependent RNA polymerase and host translation elongation factor 1A. Virology **347:** 100–108.

Yamaji, Y., et al. (2012). Lectin-mediated resistance impairs plant virus infection at the cellular level. Plant Cell **24:** 778–793.

Ye, K., Malinina, L., and Patel, D.J. (2003). Recognition of small interfering RNA by a viral suppressor of RNA silencing. Nature **426:** 874–878.

Yoshikawa, M., Iki, T., Tsutsui, Y., Miyashita, K., Poethig, R.S., Habu, Y., and Ishikawa, M. (2013). 3′ fragment of miR173-programmed RISC-cleaved RNA is protected from degradation in a complex with RISC and SGS3. Proc. Natl. Acad. Sci. USA **110:** 4117–4122.

Yoshikawa, M., Peragine, A., Park, M.Y., and Poethig, R.S. (2005). A pathway for the biogenesis of trans-acting siRNAs in Arabidopsis. Genes Dev. **19:** 2164–2175.

Zhang, X., Yuan, Y.R., Pei, Y., Lin, S.S., Tuschl, T., Patel, D.J., and Chua, N.H. (2006). Cucumber mosaic virus-encoded 2b suppressor inhibits Arabidopsis Argonaute1 cleavage activity to counter plant defense. Genes Dev. **20:** 3255–3268.

Zheng, Q., Ryvkin, P., Li, F., Dragomir, I., Valladares, O., Yang, J., Cao, K., Wang, L.S., and Gregory, B.D. (2010). Genome-wide double-stranded RNA sequencing reveals the functional significance of base-paired RNAs in Arabidopsis. PLoS Genet. **6:** e1001141.